Chemical Geology 459 (2017) 75–90

Contents lists available at ScienceDirect

Chemical Geology

journal homepage: www.elsevier.com/locate/chemgeo

Microbe-clay interactions as a mechanism for the preservation of organic matter and trace metal biosignatures in black shales

Tiffany Playter[a,*], Kurt Konhauser[a], George Owttrim[a], Cheryl Hodgson[a,1], Tyler Warchola[a], Aleksandra M. Mloszewska[a,2], Bruce Sutherland[a], Andrey Bekker[b], J.-P. Zonneveld[a], S. George Pemberton[a], Murray Gingras[a]

[a] Department of Earth and Atmospheric Sciences, University of Alberta, Edmonton, Alberta T6G 2E3, Canada
[b] University of California at Riverside, Riverside, CA 92521, USA

ARTICLE INFO

Keywords:
Microbes
Black shale
Organic-matter
Kaolinite
Montmorillonite
Flocculation
Anoxia

ABSTRACT

Organic-rich, fine-grained sedimentary rocks, such as black shales, are important geochemical archives providing information on the evolution of seawater composition and biological activity over the past 3 billion years. While biological productivity and sedimentation rates greatly affect the organic matter content in these rocks, mechanisms linking these two processes remain poorly resolved. Here, we examine the interactions of clay minerals with the marine planktonic cyanobacterium *Synechococcus* sp. PCC 7002. We suggest that clays settling through the water column could influence carbon and trace metal burial in three ways: (1) the interaction of reactive clay surfaces with the bacterial cells increases organic matter deposition via mass increase in a seawater growth medium by several orders of magnitude; (2) reactive bacterial cells become completely encased within a clay shroud, enhancing the preservation potential of this organic matter; and (3) the trace metal content of the biomass buried along with metals sorbed to the clay particles contributes to the trace metal concentrations of the black shale precursor sediments. Significantly, our findings imply that the chemical composition of ancient, organic-rich, fine-grained deposits are not only archives of ancient seawater composition and redox state, but they also provide a record of the degree of biological activity in the water column through geological time.

1. Introduction

The lithology of organic-rich, black shales consist of quartz, feldspars, carbonates, sulfides, clay minerals, and at least 1 wt% organic material (Arthur and Sageman, 1994; Aplin and Macquaker, 2011). The organic-rich nature of these rocks requires one of, or a combination of, the following conditions: (i) high primary production rates in the water column (Macquaker et al., 2010), (ii) sedimentation rates high enough to induce rapid burial of organic matter (Betts and Holland, 1991; Canfield, 1994; Tyson, 2001), and/or (iii) low organic matter respiration rates (Smith and Hollibaugh, 1993; Kristensen, 2000; Piper and Calvert, 2009). The latter can occur in several ways, including: (i) limited aerobic respiration due to low O_2 penetration into the sediment (Kristensen, 2000); (ii) reduced anaerobic respiration due to a lack of pore-water sulfate (Canfield et al., 1993a, 1993b); or (iii) the sorption of organic material onto clay particles in the water column preventing its degradation by heterotrophic bacteria (Pedersen and Calvert, 1990; Hedges and Keil, 1995; Ransom et al., 1997, 1998; Bennett et al., 1999; Lünsdorf et al., 2000; Tyson, 2001; Kennedy et al., 2002; Macquaker et al., 2010; Aplin and Macquaker, 2011).

In recent years, black shale deposits have been studied extensively to interpret the seawater trace metal concentrations and redox state of the ancient oceans and atmosphere (e.g., Tribovillard et al., 2006; Anbar and Rouxel, 2007; Scott et al., 2008, 2013; Partin et al., 2013; Reinhard et al., 2013; Swanner et al., 2014). This is because the size of a given trace metal seawater reservoir is determined by the weathering flux from land and the relative influence of the sulfidic and oxic sinks (e.g., Algeo and Maynard, 2004; Scott et al., 2008). Moreover, the clay and organic fractions in these fine-grained sediments are highly reactive, and as such, they capture and preserve the trace element availability in the seawater from which the aggregates settled.

Planktonic cyanobacteria, such as *Synechococcus* and

* Corresponding author.
E-mail address: tdavies@ualberta.ca (T. Playter).
[1] Present address: Simon Fraser University, Burnaby, British Columbia V5A 1S6, Canada.
[2] Present address: Earth Sciences Department, University of Toronto, Toronto, Ontario M5S 3B1, Canada.

http://dx.doi.org/10.1016/j.chemgeo.2017.04.007
Received 5 May 2016; Received in revised form 5 April 2017; Accepted 8 April 2017
Available online 17 April 2017
0009-2541/

Prochlorococcus, are widely distributed throughout the ocean and can occur in cell densities ranging from 10^3 to 10^8 cells per milliliter, with the highest concentrations occurring during the summer months (e.g., Waterbury et al., 1979; Miyazono et al., 1992; Jacquet et al., 1998; Ohkouchi et al., 2006). They have been observed to contribute significantly to the carbon biomass of the water column, and in some cases, they constitute the majority of the biomass (Campbell et al., 1997). Indeed, biomarker analysis (indicating the presence of 2-methylhopanoids or their diagenetic derivatives, C_{35} homohopanoids) and stable carbon isotopic signatures suggest that cyanobacteria have been major contributors to shale deposition from the Neoproterozoic through to the Phanerozoic (Bechtel and Püttmann, 1997; Köster et al., 1998; Kuypers et al., 2004; Dumitrescu and Brassell, 2005; Olcott et al., 2005; Ohkouchi et al., 2006; Duque-Botero and Maurrasse, 2008; Kashiyama et al., 2008). Recent studies have also demonstrated that planktonic cyanobacterial cell surfaces are highly reactive (Lalonde et al., 2008a, 2008b; Liu et al., 2015) and thus capable of accumulating trace metals from solution (e.g., Dittrich and Sibler, 2005; Hadjoudja et al., 2010). That same reactivity has also been shown to facilitate the adsorption of detrital clay particles and the nucleation of authigenic clay phases (e.g., Konhauser et al., 1993, 1998). In this regard, we propose that live, planktonic cyanobacteria (and indeed any reactive microbial cell), such as *Synechococcus*, could increase clay flocculation, thereby facilitating more rapid deposition of cell-clay aggregates to the seafloor. If rapid burial promotes greater preservation of organic carbon, then this mechanism may very well underpin the formation and preservation of black shale deposits in the rock record, and explain their enrichment in trace metals (e.g. Calvert and Pedersen, 1993; Algeo and Maynard, 2004) as being sourced from the remnants of cell biomass. Furthermore, the increased preservation potential of these cell-clay aggregates suggests that the trace metal signatures of reactive bacterial biomass may become incorporated into the sediments over geologic time-scales.

We test this hypothesis by: (1) observing the depositional rates of *Synechococcus* in the presence of clay (kaolinite and montmorillonite); (2) assessing if clay deposition is influenced by cell metabolism; (3) determining the morphology of the clay-cell aggregates and their preservation potential; and ultimately (4) measuring the trace element composition of *Synechococcus* for the purpose of defining their contribution to the trace metal composition of black shales. These clays were chosen because they are common in near-shore, marine (kaolinite; Thiry, 2000) and fluvial/deltaic (montmorillonite; e.g., Taggart and Kaiser, 1960) environments and encompass both a 1:1 (kaolinite) and 2:1 (montmorillonite) tetrahedral structure. Importantly, these clays encompass a range of structural composition and environments of natural occurrence.

2. Methods

2.1. Culturing

Flocculation experiments (n = 18) were performed using *Synechococcus* sp. PCC 7002 (hereafter simply referred to as *Synechococcus*), a sheathless, planktonic, coccoid marine species. Axenic populations were grown in liquid A + media (Stevens and Porter, 1980), while stock populations were maintained on A + agar plates at 30 °C. Experimental cultures were grown in liquid media, shaken at 150 rpm and bubbled with filtered and humidified air (Chamot and Owttrim, 2000). Growth was monitored by measuring optical density at 750 nm and chlorophyll *a* (Chl *a*) concentration, as described by Sakamoto and Bryant (1998). Chl *a* concentration was calculated using the formula (Porra et al., 1989):

Chl $a = 16.29OD_{665} - 8.54OD_{652}$. Cell concentration, in grams, were calculated using an additional conversion factor of 7.4×10^{10} cells/L = 10 g/L (Liu et al., 2015). Initial concentrations before clay addition (time −1 on the x-axis of Fig. 1) for all experiments involving kaolinite and montmorillonite were determined using a conversion factor (Liu et al., 2015), to calculate initial cell concentration from OD_{750} nm measurements. This was done to ensure repeatability, as the measurement of OD_{750} nm can be accurately measured during culturing. Cultures were killed by autoclaving for 60 min at 121 °C at 18 psi.

2.2. Flocculation experiments

Eighteen experiments were performed with both live and heat-killed biomass in order to ascertain whether metabolic activity was the main driver of clay flocculation and to determine whether surface charge continued to facilitate flocculation after cell lysis. Kaolinite $[Al_2Si_2O_5(OH)_4]$ (K Ga-2 from the Source Clay Repository of the Clay Minerals Society; sourced from Warren County, Georgia, USA) was used in this study because it is a common 1:1 clay mineral in which the stacked tetrahedral sheet (Si-O tetrahedrons) are hydrogen bonded directly to the octahedral sheet (mainly Al-O octahedrons) through the sharing of oxygen atoms between silicon and aluminum atoms in adjacent sheets. There is almost no substitution of Al^{3+} for Si^{4+}, or Mg^{2+} for Al^{3+}, therefore, their net surface charge is low (e.g., Ikhsan et al., 1999). Kaolinite is a stable product of either prolonged continental weathering or intense chemical weathering in humid tropical environments, and thus it accumulates in a number of near-shore, marine depositional environments (Thiry, 2000).

Montmorillonite $[(Na,Ca)_{0.33}(Al,Mg)_2(Si_4O_{10})(OH)_2{\cdot}nH_2O]$ (SWy-2; Na-rich montmorillonite from Cook County, Wyoming, USA) was also used because it is a common 2:1 clay mineral that consists of two tetrahedral sheets bound to either side of an octahedral sheet (dioctahedral aluminum hydroxide). The structural composition of the sheets allows isomorphic substitutions by lower charge cations, which generates a net negative layer charge and leads to strong colloidal characteristics (e.g., Thomas et al., 1999). Montmorillonite is a common constituent of fluvial and deltaic clay, particularly in catchments with volcanic rocks, such as the Mississippi River (e.g., Taggart and Kaiser, 1960).

During each experiment, a 400 mL cyanobacterial culture was first diluted with A + media to create a 1 L volume. A + media was generated using a standard formulation (A + Medium Recipe, 2017) based on the work of Stevens and Porter (1980) and McClure et al. (2016). Compared to seawater (at 500 mM NaCl salinity), this media has slightly lower concentrations of cations (e.g. 300 mM NaCl and 8 mM KCl; Ludwig and Bryant, 2012). The diluted bacterial culture was incubated in an acrylic 5.1 cm × 20 cm tank in front of a bank of fluorescent lights in a curtained enclosure (see Sutherland et al., 2014 for experimental setup) at room temperature. Clay (kaolinite or montmorillonite) was added to a final concentration of 0.1 g/L, 5 g/L and 50 g/L, chosen to represent the spectrum of suspended load observed in modern estuaries (Kistner and Pettigrew, 2001; Uncles et al., 2006). The mixture was vigorously stirred to produce a semi-homogeneous mixture, and a HD video camera was used to record each experiment. Sampling for Chl *a* concentrations commenced immediately following clay addition and subsequently at 5, 10, 15, 30, 90, 120, 180 and 240 min.

Controls were performed to independently measure the settling rates of the *Synechococcus* in the absence of clay. Additionally, similar controls were used to measure the rate of clay sedimentation in growth media. To rule out the role of suspended load (resulting in lack of light penetration) on cyanobacterial sedimentation by affecting cell metabolism, an additional tank experiment was conducted whereby *Synechococcus* sedimentation rate (via Chl *a* measurements) was measured over time in complete darkness. During this treatment, all the lights were turned off, the blinds were drawn, and the tank was covered with a black shroud. The chemical behavior of heat-killed *Synechococcus* biomass compared to live cultures also addresses the effect of turbidity (and inferred cell-death) on sedimentation. If both

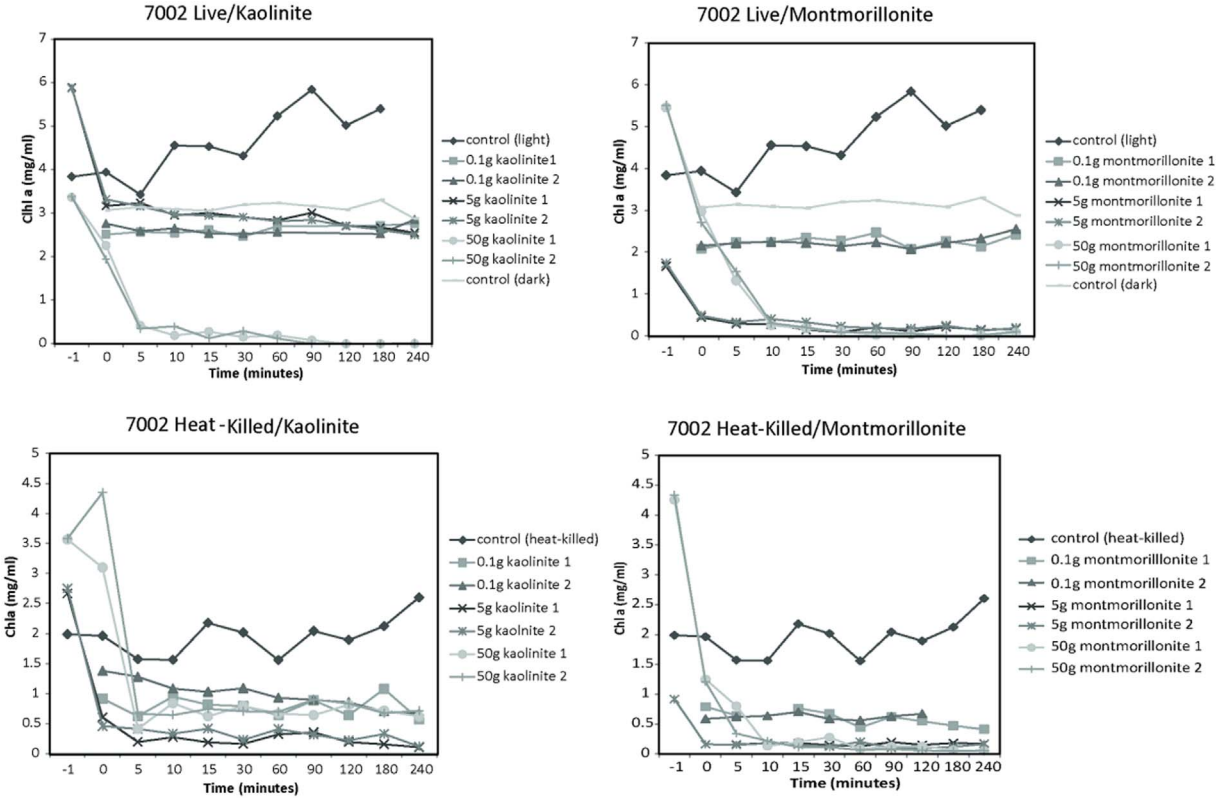

Fig. 1. Quantification of *Synechococcus* sedimentation. Graphical representation of the measured decline of Chl *a* over time after kaolinite or montmorillonite was added in varying volumes (0.1 g, 5 g or 50 g) to live or dead *Synechococcus* cells. Time −1 represents initial cell concentration before clay addition. Time 0 represents cell concentrations immediately following clay addition. Controls included were: *Synechococcus* under normal growth conditions (light), *Synechococcus* under stressed conditions (darkness) and dead *Synechococcus* over time (dead).

live and heat-killed biomass behave in a similar chemical manner, cell death due to turbidity would not be a factor.

2.3. Trace metal analysis

The trace metal composition of *Synechococcus* was measured using a 1 mL volume with a cell concentration of 3.8×10^7 cells/mL. Analyte values were measured in triplicate for cyanobacteria in growth media (A +) and compared with the average values of A + media alone (see Table 1 for original data and detection limits; refer to Table 2 for averaged data). The difference between these two values was taken to be the analyte contribution. Trace metal concentrations within a 1 L volume were calculated using two cyanobacterial concentrations that represent both ideal experimental conditions and the modern oceans: (1) the measured bacterial concentration of 3.8×10^7 cells/mL (5.14 g/L wet weight) and (2) the concentration of *Synechococcus* reported by Campbell et al. (1997; Table 2), with values of 10^3 cells/mL (1.35×10^{-4} g/L wet weight).

Trace metal concentrations were obtained by analyzing samples in triplicate using a Perkin Elmer Elan 6000 quadrupole inductively coupled plasma mass spectrometer (ICPMS) following acid digestion (Nuester et al., 2012). The instrument was calibrated using 5 certified multi-element solutions (CPI International), and instrument drift was corrected using In, Bi, and Sc as internal standards. Running conditions were: a flow rate of approximately 1 mL/min, 35 sweeps/reading, 1 reading/replicate and 3 replicates. Dwell times of 10 ms were used for Na, Al, K, Cu, Zn and Sr and 150 ms for Se. The dwell times of other elements were 20 ms. The integration time (dwell time multiplied by the number of sweeps) was 350 ms for Al, K, Cu, Zn, and Sr; 5250 ms for Se; and 700 ms for the remaining elements. The final results are the average of 3 replicates. The instrument was set in dual detector mode with the ICP RF power set to 1300 W. Measurements were taken in counts per second (cps) and the blank values were subtracted after the internal standard correction. The auto lens function was turned on and 4 point calibration curves were used (0, 0.25, 0.50, 1.00 ppm for Na, Ca, Mg, Fe, K and P; 0, 0.005, 0.010 and 0.020 ppm for the remaining elements).

Table 1
Raw ICP-MS data of cyanobacterial cells and A + media composition. All data is reported in ppm. A- denotes A + media values only; S11- denotes cyanobacterial cells in A + media mixture. The value < DL represents a value below detection limits. Elements that occurred below detection limits in both cyanobacterial cells and A + media include: Be, Ga, Ge, As, Se, Y, Zr, Nb, Mo, Ru, V, Pd, Ag, Cd, Sn, Sb, Te, Cs, La, Ce, Pr, Nd, Sm, Eu, Gd, Tb, Dy, Ho, Er, Tm, Yb, Lu, Hf, Ta, W, Re, Os, Ir, Pt, Au, Tl, Pb, Th, and U.

Analyte	Detection limits (DL)	Units	A-1	A-2	A-3	S11-6	S11-7	S11-8
Li	0.005	ppm	< DL	0.0060	< DL	0.0070	< DL	< DL
B	0.2	ppm	3.4	3.7	3.8	4.1	5.4	4.9
Na	0.05	ppm	7232	7324	7362	7352	9261	8662
Mg	0.2	ppm	461	471	484	509	630	587
Al	0.02	ppm	0.22	0.22	0.19	0.20	0.20	0.23
P	0.5	ppm	7.9	7.8	7.9	11.3	13.9	12.7
K	0.6	ppm	307	310	318	333	423	394
Ca	3.1	ppm	53.1	52.4	53.8	59.6	75.4	70.3
Ti	0.009	ppm	0.037	0.039	0.040	0.041	0.053	0.054
Cr	0.005	ppm	0.440	0.239	0.238	0.239	0.243	0.244
Fe	0.37	ppm	1.65	0.936	0.732	0.461	0.317	< DL
Mn	0.003	ppm	1.24	1.23	1.25	1.22	1.50	1.39
Co	0.003	ppm	0.023	0.023	0.022	0.015	0.017	0.016
Ni	0.006	ppm	0.406	0.362	0.359	0.357	0.348	0.354
Cu	0.003	ppm	0.281	0.264	0.263	0.260	0.294	0.285
Zn	0.008	ppm	0.515	0.517	0.531	0.500	0.557	0.579
Rb	0.004	ppm	0.012	0.012	0.012	0.025	0.032	0.030
Sr	0.003	ppm	0.027	0.028	0.028	0.034	0.040	0.037
Ba	0.003	ppm	0.005	0.013	0.006	0.009	0.008	0.009

Table 2
Averaged ICP-MS results in ppm.

Analyte	Li	B	Na	Mg	Al	P	K	Ca	Ti	Cr	Fe	Mn	Co	Ni	Cu	Zn	Rb	Sr	Ba
Detection limits (DL)	0.005	0.200	0.050	0.200	0.020	0.500	0.600	3.100	0.009	0.005	0.370	0.003	0.003	0.006	0.003	0.008	0.004	0.003	0.003
Bacteria in media avg	0.007	4.776	8425	575.3	0.211	12.62	383.4	68.43	0.049	0.242	0.389	1.371	0.016	0.353	0.279	0.546	0.029	0.037	0.009
A + avg	0.006	3.661	7306	471.9	0.212	7.853	311.5	53.11	0.039	0.306	1.107	1.238	0.023	0.376	0.269	0.521	0.012	0.028	0.008
Bacterial contribution	0.001	1.116	1119,050	103.444	0.00	4.769	71.848	15.321	0.010	0.00	0.00	0.133	0.00	0.00	0.010	0.024	0.017	0.009	0.001
Value for 3.8 × 10^10 cells/L	1.005	1116	1,119,050	103,444	0.00	4769	71,848	15,321	10.453	0.00	0.00	133.42	0.00	0.00	10.32	24.37	17.04	9.48	0.70
Value for 10^6 cells/L	0.0001	0.1116	111.9	10.34	0.00	0.477	7.18	1.532	0.001	0.00	0.00	0.0133	0.00	0.00	0.001	0.0024	0.0017	0.0009	0.0001
Amount (μg/L)	100	111,572	111,905,010	10,344,397	0.00	476,917	7,184,778	1,532,113	1045	0.00	0.00	13,341.99	0.00	0.00	1031.66	2436.71	1703.65	947.68	69.52

2.4. TEM and SEM imaging

Synechococcus was imaged using transmission electron microscopy (TEM) and scanning electron microscopy (SEM). For both SEM and TEM imaging, *Synechococcus* cells were fixed over the course of 2 h at room temperature in a mixture of 2.5% glutaraldehyde, 2% paraformaldehyde, and 0.1 M phosphate buffer. If necessary, the fixed cells were stored in a refrigerator overnight at 4 °C. After fixation, cells were centrifuged at 10,000 rpm, and rinsed 3 × in 0.1 M phosphate buffer saline (PBS) to remove excess fixative.

For SEM imaging, fixed cells were rinsed 3 × in 0.1 M PBS and dehydrated through a graded ethanol series as for TEM sample preparation. Additional dehydration steps were performed in which cells were placed into mixtures of ethanol and hexamethyldisilazane (HMDS) (75:25, 50:50, 25:75), and finally left in 100% HMDS overnight. Dehydrated cells were dried in a desiccation chamber overnight, placed on aluminum SEM stubs and sputter-coated with gold. A Philips FEI XL30 SEM operating at 20 kV was used to image the cells.

Preparation of samples for SEM imaging of *Synechococcus* associated with clay was carried out by mixing a 1 mL aliquot of the A + medium cell suspension with 1 mg, 10 mg, and 25 mg of kaolinite and montmorillonite, before following the generic SEM procedure described above. The procedure for TEM imaging of the clay-cyanobacterial mixtures was simplified by eliminating all dehydration processing, and simply placing a drop of the fixative containing the bacteria clay mixture onto a TEM grid, and staining with 1% osmium tetroxide. This was done to limit the amount of sample processing that could potentially affect the interaction of the clay and bacteria to provide the most accurate representation of the natural association between the clay and bacteria. In subsequent control experiments, sampling through the entire dehydration process, including multiple centrifugations and re-suspensions, was not observed to significantly affect the resulting clay-bacteria interaction. Again, separate samples were prepared that contained 1 mg, 10 mg, and 25 mg of kaolinite and montmorillonite, in an effort to capture any variation in clay-bacterial interactions dependent on clay concentration.

3. Results

3.1. Chl a measurements

Fig. 1 shows concentrations of the photosynthetic pigment Chl *a* over 18 successive 240-minute growth experiments with *Synechococcus* supplemented with either kaolinite or montmorillonite clay. Chl *a* concentration was used as a measure of cyanobacterial abundance remaining 5 cm below the water surface. In control samples (non-clay supplemented cultures), Chl *a* increased over time, as would be expected from the cells in exponential growth phase (Fig. 1), or, in the case of darkness, remained constant. In contrast, Chl *a* concentrations of kaolinite/montmorillonite-supplemented *Synechococcus* cultures showed either unchanging or declining levels at all clay concentrations tested (Fig. 1). For both clays, the rate of decrease in Chl *a* concentration accelerated as the clay concentration increased (Fig. 1). Photographs of representative sedimentation time intervals are shown in Fig. 2. These provide visual representation that the clay-cyanobacterial mixtures rapidly deposit from the water column, and at a rate that increased with increasing clay concentration.

Heat-killed *Synechococcus* biomass reacted similarly to live cultures, showing a decrease in Chl *a* concentration over time when 5 g or 50 g of kaolinite or montmorillonite was added (Fig. 1). This is in contrast to the live *Synechococcus* control culture kept in complete darkness. The addition of 0.01 g of kaolinite or montmorillonite induced a gradual drop in Chl *a* levels, however, Chl *a* levels fluctuated more in the presence of montmorillonite. The addition of 50 g of kaolinite or montmorillonite induced a sharp drop in Chl *a* levels in dead population of *Synechococcus*.

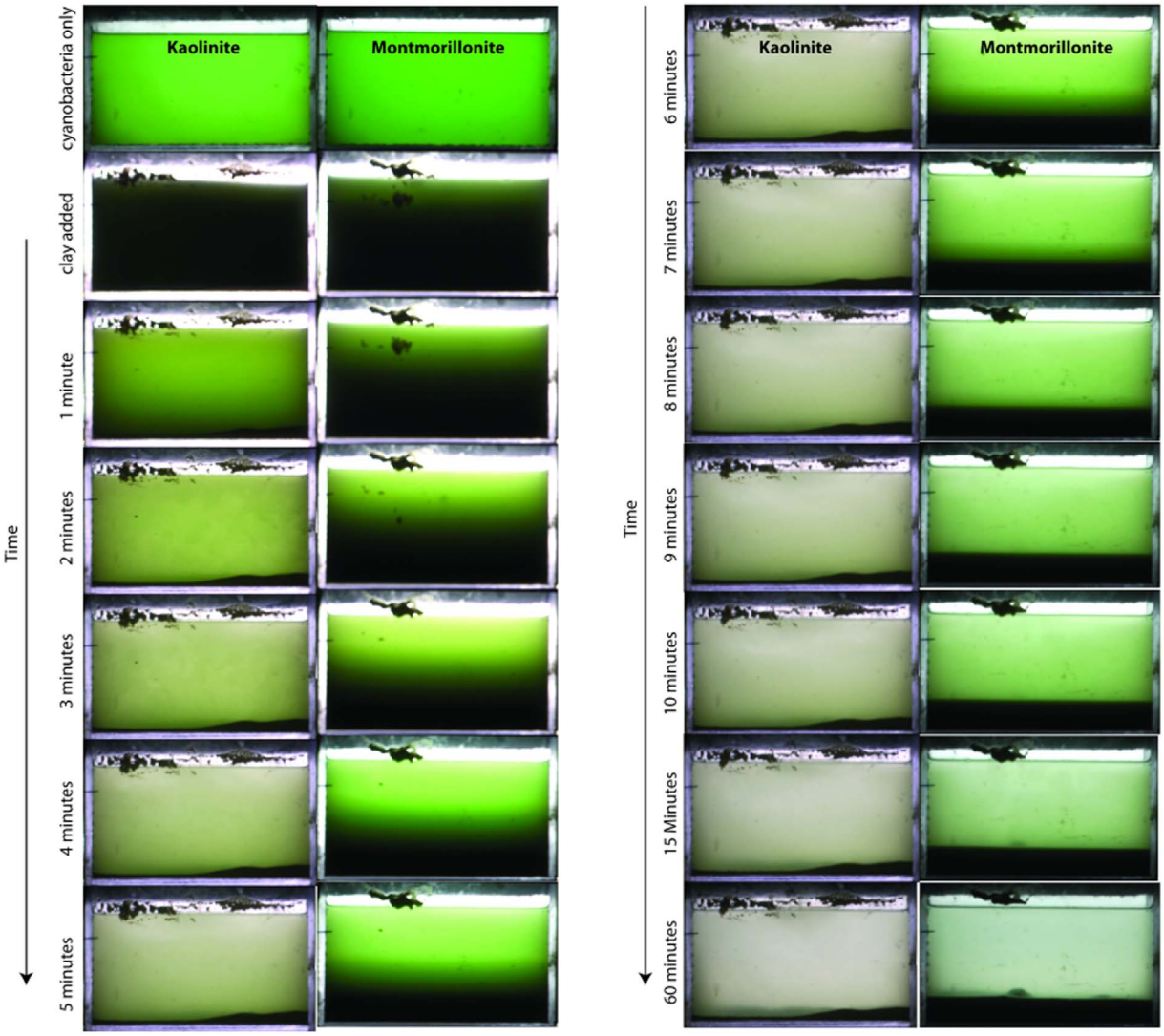

Fig. 2. Time course of representative experimental sedimentation tanks illustrating *Synechococcus*-clay deposition. Kaolinite and montmorillonite (50 g) were added to 1 L volume of cyanobacteria. Images include kaolinite-*Synechococcus* and montmorillonite-*Synechococcus* mixtures for comparison. Note that within 15 min, the kaolinite-*Synechococcus* mixture is largely settled, creating a pale green/grey mass at the bottom of the tank. (For interpretation of the references to color in this figure legend, the reader is referred to the web version of this article.)

Overall, the trends that we observe pertaining to the live cultures, include: (i) 0 mg/mL of Chl *a* after 10 min when 50 g of kaolinite or montmorillonite is added, (ii) the addition of small amounts of kaolinite, or montmorillonite (0.01 g) produced minimal deviation from the controls. Data from the heat-killed *Synechococcus* biomass are similar to that obtained from the live cultures. Calculated initial cell concentrations for experiments (using OD_{750} conversion factor from Liu et al. (2015)) involving kaolinite and montmorillonite (time − 1 on the x-axis of Fig. 1) may be overestimated when compared to the graphical average trend.

3.2. SEM/TEM results

Using SEM imaging, we observed that *Synechococcus* cells, grown under normal conditions in A + media, are typically spherical to ovoid, unicellular and average 1 μm in diameter, but clump together to form larger cell aggregates (Fig. 3A). The intracellular structures, including the thylakoid membrane and nucleotide, are visible using TEM (Fig. 3B).

SEM analysis of *Synechococcus*-kaolinite (Fig. 4A–D), and *Synechococcus*-montmorillonite (Fig. 4E–H) mixtures clearly indicates that the cells are encrusted with clay. In addition, the kaolinite and montmorillonite-encrusted cells frequently adhere to larger kaolinite or montmorillonite structures to become amorphous masses of cell-clay aggregates whose sizes exceed tens of micrometers (Fig. 4D). When exposed to kaolinite, *Synechococcus* cells become encrusted in micron-sized, plate-like features that generally conform to the morphology of the cyanobacterial cells (Fig. 4A–C). Where hexagonal grains encrusting cyanobacterial cells are discernible, the clay mineral face (the region of largest surface area) appears to be the point of contact with the bacterial cell, while the clay mineral edge (region of small surface area) is the point of contact with other clay mineral grains (Fig. 4A–C).

TEM analysis of *Synechococcus*-kaolinite mixtures reveals the formation of thick kaolinite sheaths, which can be over 1 μm thick, encasing individual cyanobacterial cells (Fig. 5A–B). Imaging of *Synechococcus* in the absence of clay clearly shows extracellular structure such as fimbriae (Fig. 5C). Additionally, when kaolinite is present, the encapsulation of multiple cells is visible (Fig. 5D–E).

Sheet-like structures are common and can be laterally extensive (Fig. 4A). In detail, the kaolinite is seen as hexagonal platelets, with an edge-to-edge (E-E) contact between grains (Fig. 4A). This E-E contact facilitates the formation of large sheet structures (e.g. Du et al., 2009). The kaolinite also forms larger, nodular branching structures (Fig.4D). Stacked kaolinite grains can be seen forming aggregates, which

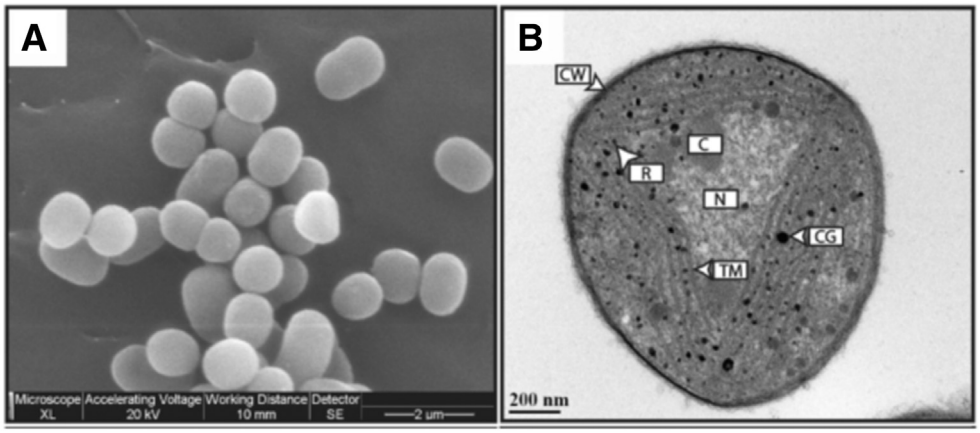

Fig. 3. Electron microscopic images showing the ultrastructure of *Synechococcus* sp. PCC 7002 grown in A + medium. (A) Scanning electron microscope (SEM) micrograph showing the size and morphology of the cyanobacteria. (B) Transmission electron microscope (TEM) micrograph showing the intracellular structure, where CW, cell wall; R, ribosome; C, carboxysome; N, nucleoide region; TM, thylakoid membrane; CG, cyanophycin granule.

compared to the smooth surface of the larger nodular structure and encrusted cyanobacteria, appear rough and granular (Fig. 5B and D). In the case of these granular aggregates, contacts between kaolinite grains are not confined to grain edges only, but involve the faces of grains as well. Cyanobacterial cells are clearly visible within these aggregates (Fig. 5D, E and F). These nodular structures are also visible when examining montmorillonite-cyanobacterial aggregates (Fig. 4G and H). Upon close inspection, bacterial cells encased in montmorillonite often exhibit a rosette-structure (Fig. 4F), where some clay minerals appear to make contact with the bacterial cell and other clay mineral grains along the clay-mineral edge (edge-to-face contact). Montmorillonite grains also appear to contact the cell along the face (face-to-cell contact). Clay composition measured from *Synechococcus*-kaolinite (Fig. 6), and *Synechococcus*-montmorillonite (Fig. 7) masses are also shown.

3.3. Trace metal analysis

Raw trace metal data for all samples are listed in Table 1. The trace metal content, measured in triplicate, was averaged to determine the overall trace metal composition of *Synechococcus* cells (Table 2). Values for certain analytes are relatively high (using a cellular concentration of 10^3 cells/mL): Na (111 ppm), Mg (10 ppm), K (7 ppm), Ca (1.5 ppm), P (0.5 ppm), B (0.1 ppm) and Mn (0.01 ppm; Table 2). Elements with low cellular concentrations (< 0.01 ppm) include: Li, Al, Ti, Cr, Fe, Co, Ni, Cu, Zn, Rb, Sr and Ba (Table 2).

4. Discussion

4.1. Microbe-clay aggregation

Bacterial cells are negatively-charged over a wide range of pH due to the deprotonation of amphoteric organic ligands contained within the polymers of the cell walls (Flemming et al., 1990; Beveridge and Graham, 1991; Fein et al., 1997; Cox et al., 1999; Phoenix et al., 2002; Lalonde et al., 2008a, 2008b; Pokrovsky et al., 2008; Liu et al., 2015). These ligands bind metal cations and serve as nucleation sites for mineral authigenesis (Beveridge, 1989; Beveridge and Graham, 1991; Konhauser et al., 1994; Clarke et al., 1997). Bacteria also have the ability to partially moderate their surface charge (Doyle, 1989; Urrutia et al., 1992; Schultze-Lam et al., 1996). For instance, to generate the proton motive force, protons are continuously pumped into the fabric of the cell wall where they compete with metal cations for binding to the negatively-charged sites (e.g., Urrutia et al., 1992). This mechanism allows live bacteria to reduce detrital mineral adhesion and authigenic mineral formation on their cellular surface by filling up anionic sites with protons (Urrutia et al., 1992; Schultze-Lam et al., 1996; Konhauser and Urrutia, 1999).

The unique surface properties of the bacterial cell facilitate the formation of clay biominerals. For example, in environments where concentrations of dissolved iron proximal to the cell are greater than the solubility product of ferric hydroxide, small mineral aggregates (~100 nm) form, as iron (e.g., Fe^{3+}) initially adsorbs onto the cell surface (Konhauser et al., 1993, 1998; Konhauser and Urrutia, 1999). Additionally, pre-formed ferric hydroxide particles in suspension can be entrained by the cell (Glasauer et al., 2001). At circumneutral pH, the net positive charge of iron attracts negatively-charged counter-ions, resulting in the formation of (Fe-Al)-silicate phases via hydrogen bonding between the cell-bound iron and the dissolved aluminum, silica or aluminosilicate complexes (e.g., Davis et al., 2002). With further exposure to sufficiently concentrated solutions, poorly ordered clay phases may form as iron attached to the cell surface continues to react with negatively charged solutes (Konhauser, 2007).

In the same way, clay particles in suspension are attracted to cations because incomplete substitution, for example Al^{3+} for Si^{4+} in the tetrahedral sheet or Mg^{2+} for Al^{3+} in the octahedral sheet, results in excess negative charge on either the clay surface (exchangeable cations) or between tetrahedral sheets in 2:1 clays (interlayer cations). This negative surface charge results in a high cation-adsorption capacity for some clays (Guenther and Bozelli, 2004). The adsorption of cations to the clay (e.g., montmorillonite, kaolinite) surface results in a net-positive surface charge, which has an affinity for negatively-charged surfaces, such as bacterial cellular surfaces (Walker et al., 1989;Guenther and Bozelli, 2004). This explains the observation that, in sediments, organic matter and clay particles rarely exist in isolation, occurring instead as microaggregates (Walker et al., 1989).

Similar to the results reported here that demonstrate cyanobacterial enhancement of clay sedimentation, the adhesion of an anionic flocculent to clays in suspension has previously been observed to produce a unique structure. For instance, Du et al. (2009) observed the formation of a honeycomb network structure after the addition of the flocculent (anionic polyacrylamide copolymer FLOPAM AN-910) to a kaolinite suspension; this was not observed in the absence of the flocculent. The network observed is similar to the honeycomb structures that we observed by SEM analyses (Figs. 3 and 4) after the addition of kaolinite and montmorillonite. This suggests that, in our experiment, the bacteria themselves played the role of an anionic flocculent.

Despite previous studies showing algal cells becoming entrained in settling clay aggregates and flocculating rapidly in the presence of clay particles (e.g., Sengco et al., 2001), there is a paucity of information on the mechanisms underpinning the role of microbes, such as cyanobacteria, in clay deposition. Indeed, clay is used to control harmful algal

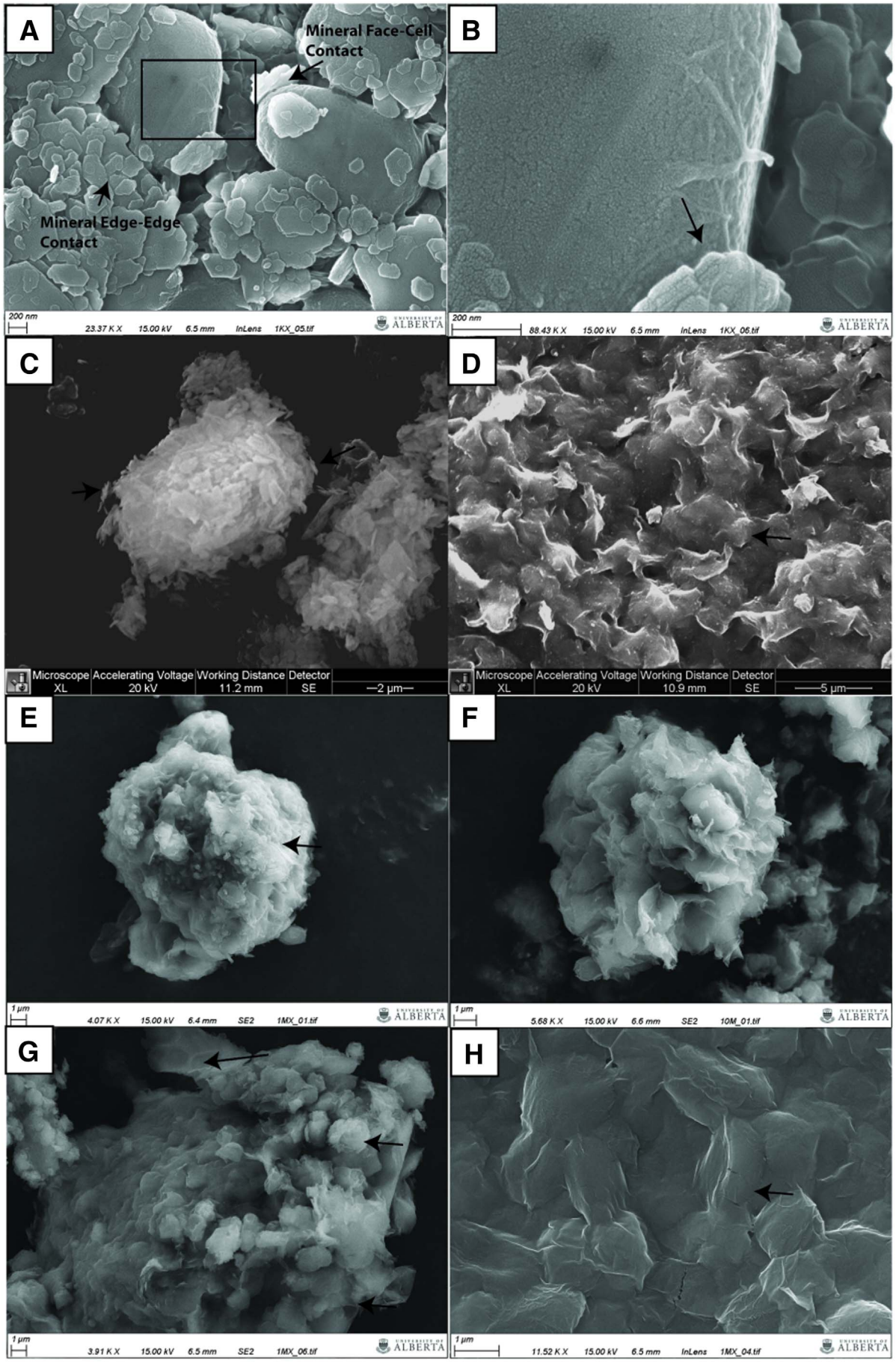

(caption on next page)

Fig. 4. Scanning electron microscope (SEM) images. (A) Kaolinite (1 mg) in the presence of *Synechococcus* sp. PCC 7002. Note the tangential attachment of the kaolinite hexagons and face-on-cell contact with the bacterial cell. Mineral edge-edge contact of kaolinite grains is also visible. Black box denotes area of inset in (B). B) Inset from (A) showing the tangential attachment of the kaolinite grain to the cell surface (contact is along mineral face). The external structure of the cell is also visible. (C) A *Synechococcus* cell encased in kaolinite. Black arrows highlight the tangential nature of mineral attachment. The cell is completely encased, however, cell morphology is preserved. (D) Large kaolinite-cell network illustrating the complete encasement of cyanobacterial cells (black arrow). Cell encasement produces a nodular morphology. (E) Cell of *Synechococcus* encased in montmorillonite. Although cell morphology is retained (black arrow), the size of the clay-cell aggregate is many times larger than an unattached cell. (F) Although tangential mineral face-to-cell contact is most common, montmorillonite can exhibit edge-to-cell contact, producing a floret-like morphology. (G) Large structure of montmorillonite and cyanobacterial cells illustrating the preservation of cell morphology and nodular textures (black arrows). (H) Complete encasement of cyanobacterial cells in montmorillonite, producing a nodular structure similar to that observed in (D).

blooms in environmental rehabilitation projects in many modern environments (e.g., Archambault et al., 2003; Beaulieu et al., 2005). The formation of clay/algal aggregates is influenced by the species of algae, clay/algae concentrations and clay type (Beaulieu et al., 2005). In the case of cyanobacteria, interaction between buoyant species, such as *Microcystis* sp., and clay particles have been observed to form aggregates that rapidly settle out of suspension (Verspagen et al., 2006). The aggregation rates of *Microcystis* sp. and clay particles are directly related to the amount of clay particles in suspension (Verspagen et al., 2006). Similarly, it has been observed that the

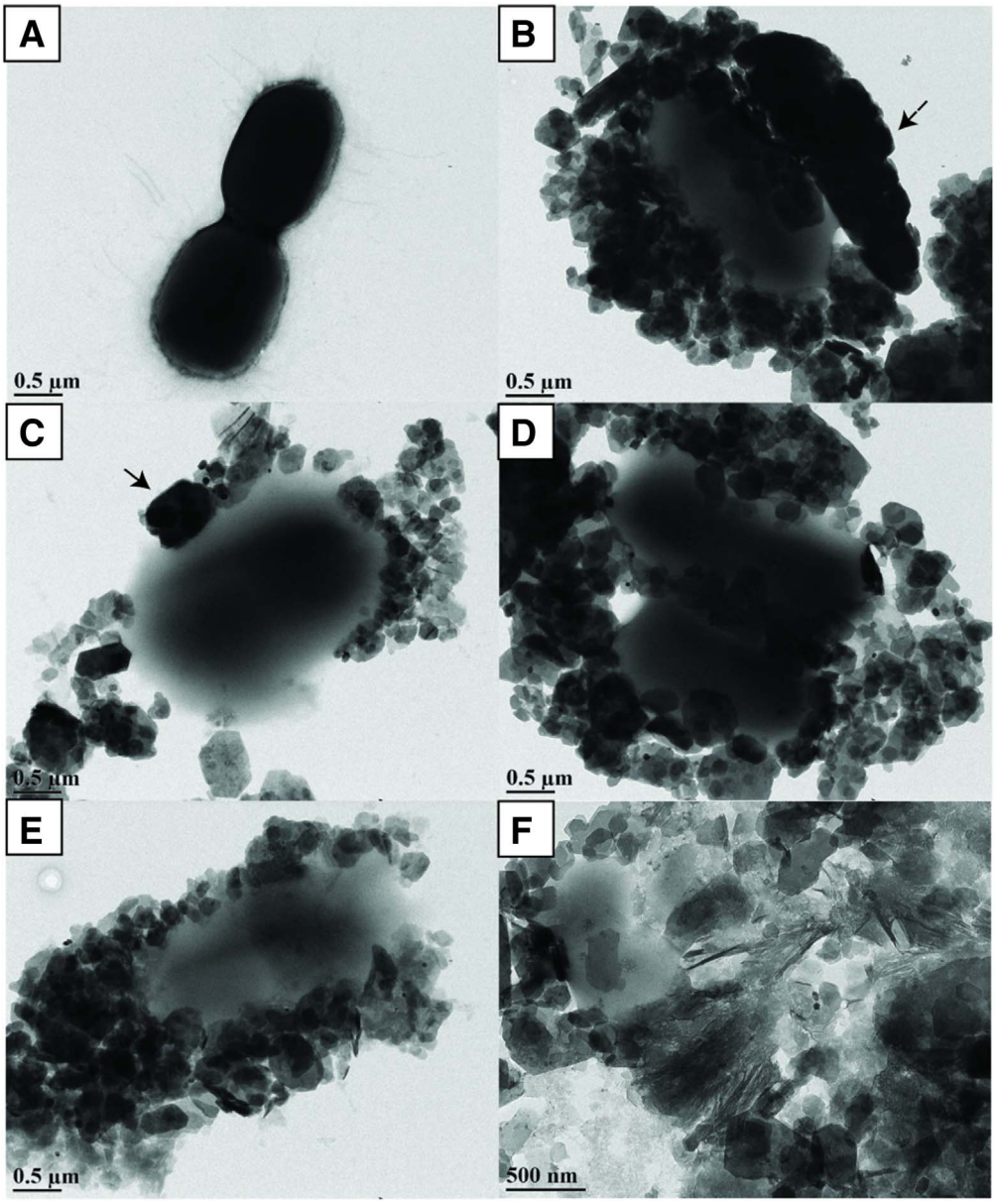

Fig. 5. Transmission electron microscope (TEM) images of kaolinite-*Synechococcus* mixtures and *Synechococcus* only. (A) Control *Synechococcus* cells dividing with no clay present. Fimbriae are clearly visible. (B) Kaolinite shells encasing *Synechococcus* cells can be thick (up to 1 µm; black arrow). (C) Kaolinite in the presence of *Synechococcus* sp. PCC 7002. Kaolinite grains can form thick stacks attached tangentially to cell, visible here with a partially covered cell (black arrows). Although the concentration of clay did not appear to influence how the bacteria sorbed to the clay in both the SEM and TEM imaging, the samples containing 1 mg of clay presented rare occurrences in which the bacteria were not completely enshrouded in clay and both the clay and bacteria were visible. This helped to provide convincing evidence that the numerous clay aggregates had a core composed of one or multiple bacteria. (D) Kaolinite grains vary in size, but form an aggregate mass partially surrounding two cells. (E) Cells of *Synechococcus* encased in kaolinite showing clay stacking. (F) Nodular, aggregate mass of bacterial cells and clay showing complete encasement of the cells.

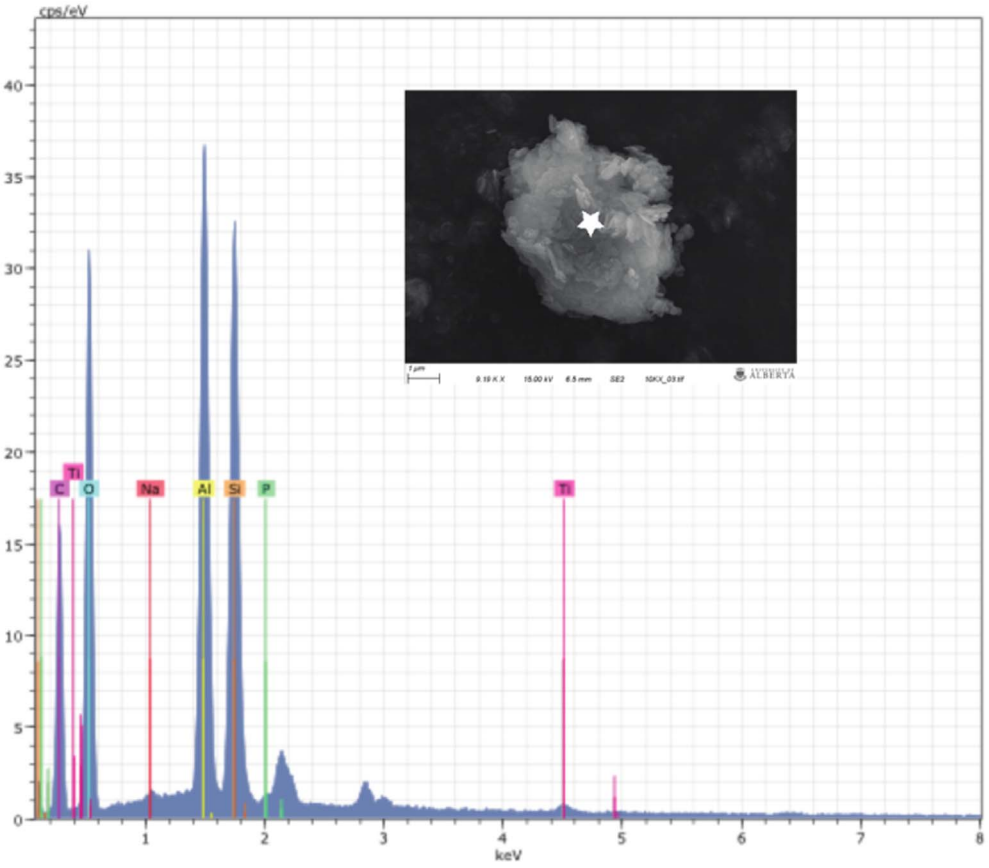

El	AN	Series	unn. C [wt.%]	norm. C [wt.%]	Atom. C [at.%]	Error (1 Sigma) [wt.%]
O	8	K-series	27.34	38.47	38.75	3.36
C	6	K-series	23.89	33.62	45.11	3.18
Si	14	K-series	9.62	13.54	7.77	0.43
Al	13	K-series	9.21	12.96	7.74	0.46
Ti	22	K-series	0.56	0.79	0.27	0.05
P	15	K-series	0.24	0.34	0.18	0.04
Na	11	K-series	0.20	0.28	0.19	0.04
		Total:	71.06	100.00	100.00	

Fig. 6. Kaolinite identification on encrusted *Synechococcus*. Insert: SEM image showing a kaolinite-encrusted cyanobacterial cell. The star indicates the point of compositional measurement. The composition of the kaolinite is shown graphically below.

sinking rates of cyanobacteria, *Anabaena* and *Phormidium*, were increased by their adhesion to clay particles (Avnimelech et al., 1982; Guenther and Bozelli, 2004). In fact, addition of clays during our experiments resulted in an increased *Synechococcus* sedimentation rate (Fig. 1). This is in agreement with the work of Verspagen et al. (2006) who observed that the aggregation rate of *Microcystis* and bentonite was linearly proportional to the concentration of clay. Additionally, Chen et al. (2010) reported that, when polysaccharide concentrations were kept constant, the flocculation efficiencies of cyanobacterial cells increased with increasing doses of kaolinite.

4.2. Organic matter sources in black shales

The organic matter found in fine-grained Triassic and Cretaceous sediments (both carbonate and siliciclastic), especially those associated with oceanic anoxic events (OAEs), have largely been attributed to cyanobacteria based on the abundance of 2-methylhopanoids, geoporphyrin distribution and nitrogen isotopic composition (Kuypers et al., 2004; Dumitrescu and Brassell, 2005; Xie et al., 2005; Ohkouchi et al., 2006; Duque-Botero and Maurrasse, 2008; Cao et al., 2009; Jia et al., 2012). For example, during the Triassic, fluctuations in the biomarker 2-methylhopane (in association with negative values of $\delta^{15}N$) have been interpreted as the products of increased cyanobacterial activity following the Permian-Triassic mass extinction, ocean anoxia, denitrification and development of oligotrophic conditions (Xie et al., 2005; Cao et al., 2009; Jia et al., 2012). Similarly, the high abundance of cholestanes suggests high rates of planktonic production in association with deposition of early Triassic, organic-rich, fine-grained successions (Suzuki et al., 1998). In Cretaceous sediments, the presence of cyanobacterial biomarkers (2β-methylhopanes and 2β-methylhopanones), in association with sterenes (indicative of algal phytoplankton), also points to a depositional environment characterized by high rates of primary, cyanobacterial production (Dumitrescu and Brassell, 2005).

In the modern oceans, cyanobacteria populations occur in densities large enough to act as major contributors to the organic fraction of marine sediments. Some species occur in concentrations as high as 10^8

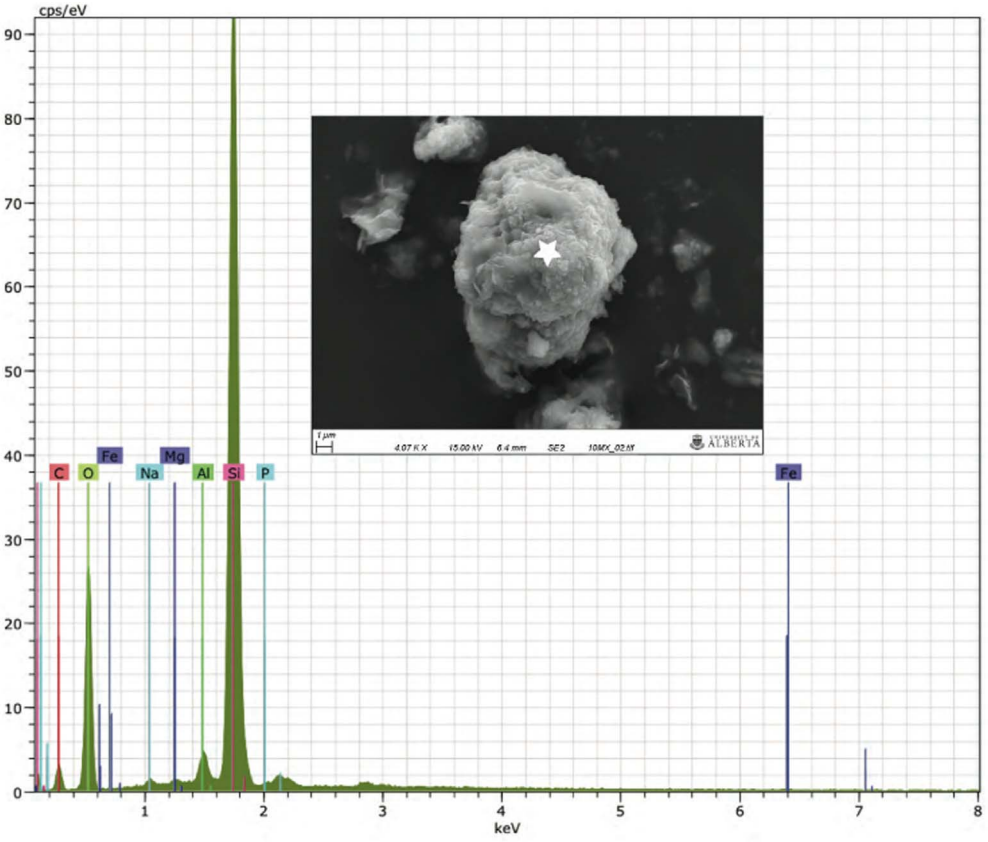

El	AN	Series	unn. C [wt.%]	norm. C [wt.%]	Atom. C [at.%]	Error (1 Sigma) [wt.%]
Si	14	K-series	40.77	45.80	31.32	1.72
O	8	K-series	32.95	37.01	44.43	4.12
C	6	K-series	12.15	13.65	21.82	2.16
Al	13	K-series	1.65	1.85	1.32	0.11
Na	11	K-series	0.52	0.58	0.48	0.07
P	15	K-series	0.37	0.41	0.26	0.05
Fe	26	K-series	0.34	0.39	0.13	0.05
Mg	12	K-series	0.28	0.31	0.25	0.05
		Total:	89.02	100.00	100.00	

Fig. 7. Montmorillonite identification on encrusted *Synechococcus*. Insert. SEM image of a montmorillonite-encased cyanobacterial cell. The composition of the clay is indicated below as measured from the point on the clay-cell aggregate indicated by the star. The composition of the montmorillonite is shown graphically below.

cells per mL (Miyazono et al., 1992). Cyanobacteria have been observed to constitute up to 70% of the total phytoplankton biomass of the northeast Atlantic Ocean (Jardillier et al., 2010). In that study, two genera of cyanobacteria, *Prochlorococcus* and *Synechococcus*, were found to contribute 45 ± 17% and 21 ± 17%, respectively, to the total carbon fixation budget for phytoplankton (Jardillier et al., 2010). In addition to high population potential, cyanobacteria occur in diverse coastal settings; by way of example, *Synechococcus* is a marine coastal genus that occurs in high cell densities within modern estuaries (Pan et al., 2007; Mitbavkar et al., 2012; Rajaneesh and Mitbavkar, 2013), making them major contributors to the estuary's organic carbon pool (Mitbavkar et al., 2012). Indeed, continental margins, where planktonic organisms flourish, have been recognized to be major sites of organic carbon deposition (Burdige, 2007).

4.3. Mechanism of biomass deposition

While the contribution of microorganisms (such as cyanobacteria) to the organic matter fraction of black shale deposits is well established, the mechanisms by which large-scale biomass deposition occurred remains extensively debated. Delivery of this reactive carbon pool to the sediment could occur rapidly (Figs. 1 and 2) via flocculation in the presence of considerable clay input. Under normal conditions, the concentration of suspended particulate matter observed in estuaries can vary considerably from 0.1 g/L in the Kennebec Estuary, USA (Kistner and Pettigrew, 2001) to over 200 g/L in the Severn Estuary, UK (Kirby and Parker, 1983; Uncles et al., 2006). Wind-delivered clay was estimated at only 6–11% of the total deposited clay (Wan et al., 2007). In some modern coastal environments, e.g., in the South China Sea, clay (smectite, illite, chlorite, and kaolinite) deposition is attributed to monsoon-induced surface currents originating from the continent (Wan et al., 2007). Considering the abundance of planktonic,

surface-reactive biomass, such as cyanobacteria, in such coastal settings, it seems plausible that microbes can accentuate mass clay settling in these environments. In fact, in an estuary exposed to seasonal monsoons, *Synechococcus* populations, for example, are shown to flourish during non-monsoonal times and diminish during monsoons due to high turbidity from the increased clay and sediment influx (Rajaneesh and Mitbavkar, 2013). Although the authors conclude that the diminished population is an effect of turbidity, in light of our observations, this population reduction may be reflective of surface-reactive, microbial populations, in this case cyanobacteria, being stripped from the water column by clay.

Considering the effect of the monsoon cycle on observed populations of *Synechococcus* (Rajaneesh and Mitbavkar, 2013), and the role of monsoons in delivering clay to the basin (Wan et al., 2007), it follows that earlier observations about the link between anomalous fluctuations in the efficiency of organic carbon burial observed in the geological record and environmental conditions (e.g., Kennedy et al., 2014) would hold true. Importantly, monsoonal control on mid-Cretaceous black shale deposition has been postulated (Herrle et al., 2003; Petrash et al., 2016). However, the authors suggested that sediment input (nutrient flux) from the monsoon promoted increased primary productivity and resulted in increased organic matter deposition and water stratification (leading to low oxygen levels and therefore an increase in organic matter preservation potential). The observation that cyanobacterial populations flourish during times of minimal surface runoff and decrease drastically because of turbidity during high monsoonal activity (Rajaneesh and Mitbavkar, 2013), contradicts this idea. In our opinion, monsoon-induced runoff would not promote an increase in primary productivity, but instead would cause the flocculation and deposition of any microorganism in suspension during that time. Combined with our results, these observations regarding clay mobilization and cyanobacterial occurrence, suggest that coastal environments (such as estuaries, prodelta settings and in proximal offshore locations), where large populations of planktonic microorganisms are present and clay input (possibly driven by monsoons) is significant, are optimal for the deposition of fine-grained, organic-rich sediment.

Although it is likely that increased monsoon-driven sedimentation into productive waters can produce high-TOC bearing stratigraphic intervals, other climatic factors may also influence microbe-mud sedimentation. High pCO_2 in the atmosphere, for example, couples increased primary productivity with enhanced clay weathering which would undoubtedly lead to widespread flocculation and settling of organic-rich mudrocks. This model explains the temporal correspondence shared by large igneous provinces and black shales (i.e. Condie, 2004).

4.4. Organic matter preservation potential

While mass organic matter deposition can occur in coastal environments, the question becomes one of preservation potential. In the oceans as a whole, < 1% of the original organic biomass buried into sediment may ultimately contribute to the sedimentary organic geochemical record (e.g., Emerson and Hedges, 1988; Raven and Falkowski, 1999). Of that fraction, most is distributed on the continental shelves because (i) there is greater nutrient supply from both land and upwelling to support primary productivity, and (ii) residence time for the dead biomass in the water column is shorter there and hence lower potential to be aerobically oxidized in the water column (Suess, 1980).

Previous studies that have focused on the preservation of microbial biomass in marine sediments showed that organic-mineral interactions result in the protection of organic matter from heterotrophic microorganisms (Hedges and Keil, 1995; Ransom et al., 1997, 1998; Bennett et al., 1999; Kennedy et al., 2002; Mayer et al., 2004; Arnarson and Keil, 2005; Aplin and Macquaker, 2011). By contrast, when separated from the host mineral grains, organic matter decays rapidly (Keil et al., 1994). This degradation occurs regardless of oxygen levels, as decomposition rates by sulfate reduction range from 65 to 85% (Mackin and Swider, 1989). Protection from degradation occurs by: (1) enclosure within pore spaces and between sheets in clay minerals (Kennedy et al., 2002; Mayer et al., 2004); (2) chemical alteration decreasing its susceptibility to chemoheterotrophy (Hedges and Keil, 1995), and (3) a lack of access to energetically favourable terminal electron acceptors (e.g., O_2, NO_3^-) for microbial respiration coupled to organic matter oxidation (see Konhauser, 2007).

The association of organic carbon with minerals, such as clay, can also protect it from bacterial enzymes and other faunal activity (Ransom et al., 1998; Baldock and Skjemstad, 2000; Bennett et al., 1999, 2012). Indeed, two mechanisms have been observed to govern organic-mineral interactions: (1) organic matter may form aggregates with mineral grains (Arnarson and Keil, 2001; Krull et al., 2003), and (2) dissolved solutes may be sorbed onto mineral surfaces (Keil et al., 1994; Baldock and Skjemstad, 2000; Ding and Henrichs, 2002). However, work thus far (e.g. Tietjen et al., 2005) has involved the use of dissolved or decaying organic matter (such as plant material). Therefore, our study shows that complete initial encapsulation of living bacterial cells during deposition is another mechanism facilitating the preservation of organic matter.

Our hypothesis builds on the work of Kennedy et al. (2002, 2014), but differs in two ways. First, those authors argued that it is dissolved organic matter in sedimentary pore fluids that results in TOC adsorption within the interlayer of smectite surfaces. By contrast, our work suggests that live particulate organic matter (such as cyanobacterial cells) can also interact with clay particles in the water column before deposition. Thus, clay flocculation is likely a combination of both these processes. Second, they suggested that the determining factor regarding organic matter preservation is mineral surface area, where dissolved organic carbon is adsorbed. While mineral surface area is certainly a critical factor (e.g., Ransom et al., 1998), we argue here that the initial encasement of particulate organic matter (such as cyanobacterial cells) by mineral grains is a driving preservational mechanism. In this regard, the surface area of the microbial cells would be of importance.

Clay minerals have been found in association with bacterial cells in modern continental margin sediments (Ransom et al., 1997). However, these microbes were observed to bind sediment using extracellular polysaccharides (EPS) and occurred in patchy distributions within the sediment or marine snow. Encasement that preserved cell morphology was not observed and organic matter was noted to occur in patchy blebs and smears (Ransom et al., 1997). While the association of these microbes with clay minerals was hypothesized to increase organic carbon preservation and sediment cohesion (even in soils; see Baldock and Skjemstad, 2000), a direct relationship between the occurrences of bacterial/cyanobacterial blooms, clay input and mass carbon deposition and preservation was not considered. Indeed, sediment trap and bottom sediment samples were not taken during a cyanobacterial bloom (Ransom et al., 1997), but during steady-state ocean conditions. In this case, the surface area of the clay minerals and the network of EPS were considered preservational factors (Ransom et al., 1997).

Baldock and Skjemstad (2000) suggested that encapsulation of organic matter in soils by clay protected the organic matter from microbial decay. Similarly, Phoenix and Konhauser (2008) suggested that the encrustation of bacteria by clay – though via biomineralization – protected the cells from toxins, dehydration and ultraviolet irradiation. Building on the work of Kilbertus (1980) and Amelung and Zech (1996), Baldock and Skjemstad (2000) hypothesized that since most bacteria cannot enter pores smaller than 3 μm (Kilbertus, 1980) and that pore size would decrease with increasing clay content in soils, aggregation and encapsulation of organic matter in soils with clay would enhance preservation. Our results show that the pore spaces associated with the clay encapsulating cyanobacterial cells are much smaller than 3 μm and, therefore, would restrict the entrance of heterotrophic microbes that would remineralize the organic matter

(Figs. 3 and 4).

Uniform clay-microbial structures ('clay hutches') have been observed to form in acidic freshwater puddles when a floating colonization surface (glass slide) is placed on the water surface and incubated (Lünsdorf et al., 2000). The work of Lünsdorf et al. (2000) showed that soil-dwelling bacteria (*Burkholderia*, *Variovorax*, *Sphingomonas*, *Rhodophila*, and *Acidobacterium*), when allowed to colonize a floating substrate (escaping high levels of toxins within the sediment) within low-pH, fresh water puddles (10–15 mm depth), will form biofilms that incorporate clay grains within the exopolymeric substances, forming clay hutches. Initial nucleation appeared to be bacterial adsorption to the substratum surface (glass slide or thin layer of extracellular polysaccharide) and subsequent coverage by clay particles adsorbed from the puddle water column. Empty/hollow clay aggregates suggested that bacteria were able to migrate within the clay aggregates. The clay hutches retained their structure upon the absence of the bacterial cell and were observed to be held together by extracellular polysaccharides. Clay particles mechanically transported from the soil to the slide (through the water column) were shown to be mechanisms of transport for adsorbed dissolved organic matter and were captured by the extracellular polysaccharides of the bacteria and incorporated into the hutch/biofilm structure. This dissolved organic matter acted as nutrients for the bacteria. These microbial-soil microhabitats were hypothesized to act as 'minimal nutritional spheres' also offering the bacterial cells protection from amoeba or flagellate grazing. These hutches were hypothesized to represent biogeological units in soils, illustrating the role of bacteria in forming clay sediments in soils.

Our work differs on two critical points as it shows: 1) complete encapsulation via direct contact between bacterial cell and clay particles (with no extracellular polysaccharide network) under marine conditions, and 2) that complete encapsulation of planktonic photosynthetic marine bacteria by clay particles brings the bacterial cells out of suspension and induces rapid deposition. In the case of the Lünsdorf et al. (2000) study, the bacteria colonized a substrate and the subsequent incorporation of clay into the bacterial biofilm added important nutrients and protection that facilitated bacterial metabolism. Additionally, the 'clay hutches' did not enclose the bacterial cells, which remained attached to the substrate.

4.5. Morphology of encased biomass

With regards to the entrapment of microorganisms, such as cyanobacteria by clay minerals, there has been limited work conducted on the morphology of these aggregates and their possible role in cellular preservation. In the case of *Anabaena*, Avnimelech et al. (1982) showed that the clay was adsorbed, forming a network-like structure around the cell perimeter, including the cell wall and EPS. Their SEM micrographs revealed that the clay occurred in clusters on the bacteria, while textures that reflected cell morphology were not produced. Studies on the flocculation of kaolinite and the diatom species *Thalassiosira punctigera* showed that the clay particles did not directly attach to the diatom cells but instead they were bound in clusters by the EPS (Hamm, 2002). Interestingly, comparison of this work with the micrographs of *Synechococcus* and kaolinite and montmorillonite aggregates from our study suggests that excessive amounts of EPS actually appeared to impede cell encapsulation. This is similar to the work of Chen et al. (2010) who showed that EPS inhibited microbe and clay flocculation.

Kim et al. (2010) also investigated the adsorption of clay minerals by the cyanobacterium, *Phormidium parchydematicum*. The clay used in that study was unspecified and was sourced from soil. Their findings showed the formation of aggregates from the attachment of clay particles to the bacterial cells. They also observed that the morphology of the cells was preserved. However, in contrast with our results, the bacterial cells were not uniformly coated, but were instead agglomerated with various clay particles of different sizes and orientation. The SEM micrographs of Kim et al. (2010) show the clay infilling spaces between the cyanobacterial filaments, but the cells themselves are not encased and instead remained partly exposed. Although we cannot demonstrate what causes the differences in aggregate textures and the ability to flocculate clay particles as observed between the various cyanobacteria and diatoms, we suggest that these varieties are a product of the composition of the EPS, and hence cell surface reactivity (*Synechococcus* vs. *Anabaena* vs. *Phormidium* or diatoms), as well as the type of clay used (kaolinite vs. montmorillonite).

4.6. Implications for traditional depositional models of black shales

The preservation of microbial organic matter via initial clay encapsulation has important implications for our understanding of the depositional mechanisms of organic-rich, fine-grained sedimentary rocks, such as black shales. High TOC content in these lithologies is not only a function of anoxia (see Arthur and Sageman, 1994), but also a function of the increased preservation potential of the microorganism, such as cyanobacteria, in the presence of a primary mineral coating such as clay. Initial encapsulation would protect the organic carbon from oxidation, regardless of pore water redox conditions, ultimately leading to the development of an organic-rich deposit. This would explain the preservation of organic matter in the presence of limited bioturbation (bioturbation suggests an oxygenated environment; see MacEachern et al., 2010; Aplin and Macquaker, 2011) in fine-grained, organic-rich sediments.

Additionally, our work suggests that sediment input of clay is crucial for the potential preservation of microbes, and so high sedimentation rates could in fact be a key mechanism for enhanced preservation of organic matter in fine-grained sediment. This complicates the view that increased sediment input dilutes the amount of organic carbon within the sediment and leads to organic-poor sediments (e.g., Aplin and Macquaker, 2011), but supports the view (Ransom et al., 1997, 1998) that sediment composition (amount of clay) is a crucial factor. Considering that, at some point, an increased sedimentation rate will dilute C_{org} content, there is likely a threshold, after which increased sedimentation rates would no longer increase C_{org} content. This threshold could be a product of both microbial cell concentration and amount of clay in suspension.

4.7. Geochemical implications for organic-rich marine shale

The increased potential for preservation when kaolinite or montmorillonite and microorganisms, such as cyanobacteria, interact has two major implications regarding elemental analysis: (1) metal cation adsorption and fractionation by clays may record, through cation bridging between the mineral and cell surfaces, a stable isotopic and/or trace metal signature not directly related to the general paleoenvironmental conditions, and (2) the trace metal content of the bacterial cells themselves has an increased likelihood of being preserved and contributing to the trace element content of the sediment. As an example of the former, Ca has been shown to fractionate by as much as −2.76‰ when adsorbing to kaolinite (Ockert et al., 2013). Compared to other clays (such as illite) kaolinite showed one of the largest Ca-isotopic fractionations. Similarly, adsorption of Mg onto kaolinite during weathering has been observed to occur with the preferential adsorption of the heavier isotope onto the clay surface (Huang et al., 2012). What is interesting is that kaolinite (and clay in general) has been observed to bind trace metals in a similar manner to metal oxyhydroxides (Spark et al., 1995), and the preferential incorporation of light Mo into secondary clay minerals has been suggested as a mechanism for the isotopic fractionation of Mo observed in riverine flux (Archer and Vance, 2008). As such, the question which remains to be addressed is whether the large fractionations of trace metals, such as molybdenum (e.g., Ellis et al., 2002; Barling and Anbar, 2004) might also be observed in association with adsorption onto kaolinite?

In a similar manner, Cr isotopes have been used as a proxy for

atmospheric oxygen levels (Frei et al., 2009; Crowe et al., 2013; Reinhard et al., 2014; Planavsky et al., 2014; Cole et al., 2016). Fractionation of Cr is thought to be controlled by redox conditions and is not currently thought to be significantly influenced by other factors, such as sorption (Ellis et al., 2002, 2004; Schauble et al., 2004; Reinhard et al., 2014). However, these studies focused on the effects of Cr absorption onto goethite (Ellis et al., 2004). Work by Buerge and Hug (1999) showed that the presence of kaolinite accelerates the reduction of Cr(VI) by Fe(II). Additionally, Cr(III) has been observed to adsorb onto kaolinite (Ajouyed et al., 2011; Rao et al., 2012). This monolayer adsorption reverses the surface charge of the kaolinite (Rao et al., 2012), which facilitates attachment to negatively-charged cyanobacterial cells. Kaolinite has been shown to absorb hexavalent Cr (Ajouyed et al., 2011) even though chromate (CrO_4^{2-}) is largely considered to be the mobile form, adsorbing to Fe(III) oxides only at acidic and near neutral pH (Izbicki et al., 2008). The adsorption of Cr (III) and Cr(VI) by montmorillonite (summarized by Bhattacharyya and Gupta, 2008), has been observed to be pH dependent. Cr(III) adsorption has been observed to increase with increasing pH, hypothesized to be a function of metal hydroxide precipitation (Bhattacharyya and Gupta, 2008). Similarly, the adsorption of Cr(VI) on kaolinite is dependent on pH, with adsorption for kaolinite peaking around pH 7.0 (Bhattacharyya and Gupta, 2008).

Further work is needed to determine the effect of kaolinite (and other clay minerals) and the adsorption of Cr (and other cations) on the isotopic signatures of black shales. The implication resulting from our work is that any isotopic signature associated with preferential adsorption onto clays would have an increased preservation potential if the element in question acted as the bridging cation between the clay mineral and microbial surfaces. This could affect any paleoenvironmental interpretations based on isotopic signatures (such as that of Cr).

Trace elements can be enriched in organic-rich shales in three ways: (1) by association with organic matter, (2) adsorption to the detrital clay fraction and (3) through incorporation into sulfide mineral phases. With respect to our data, observations support the idea that the burial of redox-sensitive metals would scale with carbon flux (Algeo and Maynard, 2004; Piper and Perkins, 2004; Dean, 2007; Reinhard et al., 2013). For instance, trace elements, such as Ni, Cd, Zn and Cu, are typically delivered to the sediments via organic matter or organometallic complexes (Calvert and Pedersen, 1993; Murphy et al., 2000; Algeo and Maynard, 2004; Piper and Perkins, 2004; Tribovillard et al., 2006). After organic matter degradation, these elements are liberated into the sediment pore-waters, and then incorporated into pyrite under reducing conditions (Brumsack, 2006; Tribovillard et al., 2006; Xu et al., 2012). This has led to the interpretation that high levels of Ni and Cu signify a high organic matter flux to the sediment and reducing conditions, allowing for the fixation of Ni and Cu into pyrite (Brumsack, 2006; Tribovillard et al., 2006).

Our findings suggest that trace metal content of microbes (specifically Mn, Cu, Zn and Ba) could contribute directly to the trace metal content of organic-rich, marine shale deposits, assuming preferential preservation of the microbial cells. A number of studies have indeed documented that marine phytoplankton are enriched in various trace elements, close to the approximate extended Redfield formula given by the following average stoichiometry (Ho et al., 2003):

$$(C_{124}N_{16}P_1S_{1.3}K_{1.7}Mn_{3.8}Mg_{0.56}Ca_{0.5})_{1000}Sr_5Fe_{7.5}Zn_{0.8}Cu_{0.38}Co_{0.19}Cd_{0.21}Mo_{0.03}$$

Although this elemental stoichiometry varies between species, growth rate, and potentially in response to ambient nutrient concentrations in seawater (Bruland et al., 1991; Twining et al., 2004), it nevertheless provides a basis for examining the magnitude by which phytoplankton may assimilate trace elements from seawater.

Second, the siliciclastic constituents can also import trace elements. For example, V has been observed to adsorb to kaolinite (Breit and Wanty, 1991). Siliciclastic input can be examined by cross-plotting the element of interest versus Al or Ti, and then comparing the ratios with average published shale values (Dean et al., 1997; Piper and Perkins, 2004; Tribovillard et al., 2006). Our findings suggest that microbial cells, specifically cyanobacteria, contribute Ti directly to the sediment, which potentially makes the normalization to Ti problematic. Additionally, while the adsorption capacity and ability of metal oxyhydroxides to bring trace metals to the sediment has been recognized, the ability of detrital clays, such as kaolinite or montmorillonite, to adsorb trace metals from the water column has been largely ignored. Our results suggest that a primary source of deposited metals originates from the bacterial cells encapsulated by clay minerals. This adds complexity to the notion that the trace element content of organic-rich deposits necessitates chemical deposition in rare environments. For example, it has been proposed that the development of euxinic conditions in the water column or at the sediment/water interface during deposition acts as a reductant for the fixation of elements such as V (Wanty and Goldhaber, 1992; Brumsack, 2006). In the case of Lower Cambrian black shale deposits from South China, high V/(V + Ni) values (above 0.85) were interpreted as indicating marine euxinia (Xu et al., 2012). However, kaolinite has been observed to adsorb V in the form of VO_3^- (Abd-Allah et al., 2005), and thus has the potential (along with other clays) to contribute to the V content of black shales (as postulated by Kelly et al., 2013). This has implications regarding global mass balance and burial models related to trace element fluxes (e.g. Reinhard et al., 2013), as the reactivity of the depositing sediment (i.e. clays) is not taken into consideration.

Although anoxia can be associated with increased primary productivity, we argue that it is the initial encapsulation of the microbial cells *en masse*, which, along with preserving the organic matter, contributes directly to sedimentary trace element concentrations. Perhaps this is an explanation for the strong association between trace elements (e.g., Cu) and TOC. Cross-plots are generally used to interpret paleoredox conditions (Tribovillard et al., 2006), but may instead reflect the enhanced preservation of marine plankton (e.g., cyanobacteria) and their trace metal components.

5. Conclusions

This study had a number of aims, one of which was to investigate the role that clay minerals have in flocculating microbial cells from suspension. The addition of montmorillonite or kaolinite (in 5 g/L or 50 g/L concentrations) to a suspension of *Synechococcus* cells was found to dramatically increase settling rates of both cells and clay; cells were brought out of suspension within 15 min. In contrast, live *Synechococcus* cells were found to increase in concentration when no clay was added. Cell metabolism was not found to be a factor as both live and dead cell populations behaved in a similar manner in the presence of clay. These findings agree with previous work which reported the ability of clay to sediment microbial cells from suspension (e.g. Beaulieu et al., 2005). As cyanobacteria have been recognized as major contributors to the organic matter content of some organic-rich marine shale deposits (Ohkouchi et al., 2006), this depositional mechanism could account for the deposition of these organic-rich shale deposits. This would suggest an environment of deposition where large microbial populations, such as cyanobacterial blooms, could occur in addition to regular clay input, such as an estuary or other coastal regions, where events such as monsoons could transport large amounts of clay to the basin. In addition, kaolinite is known to be preferentially deposited close to shore and is associated with increased continental weathering (Thiry, 2000). The increased nutrient delivery is conducive to microorganisms (e.g. cyanobacterial blooms), and, in association with the kaolinite from continental weathering, would promote the formation of organic-rich deposits. This supports deltaic, estuarine, or related depositional setting for the formation of these organic-rich deposits. Kaolinite is also stable over long periods of time (compared to other clays, such as smectite; Thiry, 2000), suggesting that long-term cyanobacterial encasement is feasible.

Clay-cell aggregates examined using SEM reveals that, in the presence of surface-reactive microbial cells (e.g. cyanobacteria), kaolinite and montmorillonite form nodular network structures that incorporate the bacterial cells. Cyanobacterial cells were completely enclosed within a clay envelope, with plates of clay visibly adhering to the negatively-charged cell surface. As the chemical reactivity of cyanobacterial cells has previously been demonstrated (Lalonde et al., 2008a, 2008b; Liu et al., 2015), this suggests that cation bridging likely occurs between the microbial and clay mineral surfaces. This mechanism potentially explains the preservation of large deposits of marine organic matter, with encapsulation of the microbes protecting the biomass from degradation.

Unsurprisingly, the trace metal content of a sample of *Synechococcus* was found to be elevated in bioactive metals (P, Cu, Zn and Ba). However, these trace metals have been thought to be largely liberated during organic matter degradation and only preserved under unique circumstances (anoxia, euxinia or increased sedimentation rates) in sediments (e.g., Algeo and Maynard, 2004; Tribovillard et al., 2006). The rapid deposition and encapsulation of cyanobacterial cells observed during our experiments does not require the development of anoxia or euxinia, suggesting that, while redox controls have been recognized to play a role in numerous organic-rich deposits, rapid deposition with encapsulation of reactive microbial biomass is another important control. This would explain the high levels of bioactive trace elements within some organic-rich deposits (e.g. Tribovillard et al., 2006). Significantly, this depositional model suggests that steady-state, organic-carbon depositional and preservation models may not be entirely accurate. Instead organic-rich, fine-grained deposits may, in some cases, reflect a series of discrete depositional events, which punctuate steady-state conditions.

Acknowledgements

This research was made possible by support received from the Natural Sciences and Engineering Research Council of Canada (165831 and 213411). AB acknowledges the support from the Society of Independent Thinkers. The authors would like to thank the following people who contributed to the work: Sarah Schultz, Denise Whitford, and Schafer Montgomery. Additional thanks are due Guangcheng Chen, at the University of Alberta, who completed all ICP-MS measurements. The authors would like to thank Arlene Oatway, Nathan Gerein, and Brendan Bishop for their aid in preparing and analyzing samples using SEM, TEM, and EDX. Lastly, the authors wish to thank two anonymous reviewers, and the Editor, whose thorough and constructive comments proved very helpful in the improvement of this manuscript. T.W. would also like to extend a special thank you to Arlene Oatway for the use of her SEM and TEM protocols, as well as the boundless patience and kindness she showed throughout their many interactions.

References

A + Medium Recipe, 2017. UTEX Culture Collection of Algae at the University of Texas at Austin. http://web.biosci.utexas.edu/utex/Media%20PDF/a%20plus%20medium.pdf (accessed 06.11.16).

Abd-Allah, S.M., El Hussaini, O.M., Mahdy, R.M., 2005. Towards a more safe environment: (4) sorptability of vanadium as a nuclear constructing material by some clay sediments in Egypt. J. Appl. Sci. Res. 1, 168–175.

Ajouyed, O., Hurel, C., Marmier, N., 2011. Evaluation of the adsorption of hexavalent chromium on kaolinite and illite. J. Environ. Prot. 2, 1347–1352.

Algeo, T.J., Maynard, J.B., 2004. Trace-element behavior and redox facies in core shales of Upper Pennsylvanian Kansas-type cyclothems. Chem. Geol. 206, 289–318.

Amelung, W., Zech, W., 1996. Organic species in ped surface and core fractions along a climosequence in the prairie North America. Geoderma 74, 193–206.

Anbar, A.D., Rouxel, O., 2007. Metal stable isotopes in paleoceanography. Annu. Rev. Earth Planet. Sci. 35, 717–746.

Aplin, A.C., Macquaker, J.H., 2011. Mudstone diversity: origin and implications for source, seal, and reservoir properties in petroleum systems. AAPG Bull. 95, 2031–2059.

Archambault, M.-C., Grant, J., Bricelj, V.M., 2003. Removal efficiency of the dinoflagellate *Heterocapsa triquetra* by phosphatic clay and implications for the mitigation of harmful algal blooms. Mar. Ecol. Prog. Ser. 253, 97–109.

Archer, C., Vance, D., 2008. The isotopic signature of the global riverine molybdenum flux and anoxia in the ancient oceans. Nat. Geosci. 1, 597–600.

Arnarson, T.S., Keil, R.G., 2001. Organic-mineral interactions in marine sediments studied using density fractionation and X-ray photoelectron spectroscopy. Org. Geochem. 32, 1401–1415.

Arnarson, T.S., Keil, R.G., 2005. Influence of organic-mineral aggregates on microbial degradation of the dinoflagellate *Scrippsiella trochoidea*. Geochim. Cosmochim. Acta 69, 2111–2117.

Arthur, M.A., Sageman, B.B., 1994. Marine black shales: depositional mechanisms and environments of ancient deposits. Annu. Rev. Earth Planet. Sci. 22, 499–552.

Avnimelech, Y., Troeger, B.W., Reed, L.W., 1982. Mutual flocculation of algae and clay: evidence and implications. Science 216, 63–65.

Baldock, J.A., Skjemstad, J.O., 2000. Role of the soil matrix and minerals in protecting natural organic materials against biological attack. Org. Geochem. 31, 697–710.

Barling, J., Anbar, A.D., 2004. Molybdenum isotope fractionation during adsorption by manganese oxides. Earth Planet. Sci. Lett. 217, 315–329.

Beaulieu, S.E., Sengco, M.R., Anderson, D.M., 2005. Using clay to control harmful algal blooms: deposition and resuspension of clay/algal flocs. Harmful Algae 4, 123–138.

Bechtel, A., Püttmann, W., 1997. Palaeoceanography of the early Zechstein Sea during Kupferschiefer deposition in the Lower Rhine Basin (Germany): a reappraisal from stable isotope an organic geochemical investigations. Palaeogeogr. Palaeoclimatol. Palaeoecol. 136, 331–358.

Bennett, R.H., Ransom, B., Kastner, M., Baerwald, R.J., Hulbert, M.H., Sawyer, W.B., Olsen, H., Lambert, M.W., 1999. Early diagenesis: impact of organic matter on mass physical properties and processes, California continental margin. Mar. Geol. 159, 7–34.

Bennett, R.H., Hulbert, M.H., Curry, K.J., Curry, A., Douglas, J., 2012. Organic matter sequestered in potential energy fields predicted by 3-D clay microstructure model, direct observations of organo-clay micro- and nanofabric. Mar. Geol. 315–318, 108–114.

Betts, J.N., Holland, H.D., 1991. The oxygen content of ocean bottom waters, the burial efficiency of organic carbon, and the regulation of atmospheric oxygen. Palaeogeogr. Palaeoclimatol. Palaeoecol. 97, 5–18.

Beveridge, T.J., 1989. Role of cellular design in bacterial metal accumulation and mineralization. Annu. Rev. Microbiol. 43, 147–171.

Beveridge, T.J., Graham, L.L., 1991. Surface layers of bacteria. Microbiol. Rev. 55, 684–705.

Bhattacharyya, K.G., Gupta, S.S., 2008. Adsorption of a few heavy metals on natural and modified kaolinite and montmorillonite: a review. Adv. Colloid Interf. Sci. 140, 114–131.

Breit, G.N., Wanty, R.B., 1991. Vanadium accumulation in carbonaceous rocks: a review of geochemical controls during deposition and diagenesis. Chem. Geol. 91, 83–97.

Bruland, K.W., Donat, J.R., Hutchins, D.A., 1991. Interactive influences of bioactive trace metals on biological production in oceanic waters. Limnol. Oceanogr. 36, 1555–1577.

Brumsack, H.J., 2006. The trace metal content of recent organic carbon-rich sediments: implications for Cretaceous black shale formation. Palaeogeogr. Palaeoclimatol. Palaeoecol. 232, 344–361.

Buerge, I.J., Hug, S.J., 1999. Influence of mineral surfaces on chromium(VI) reduction by iron(II). Environ. Sci. Technol. 33, 4285–4291.

Burdige, D.J., 2007. Preservation of organic matter in marine sediments: controls, mechanisms, and an imbalance in sediment organic carbon budgets? Chem. Rev. 107, 467–485.

Calvert, S.E., Pedersen, T.F., 1993. Geochemistry of recent oxic and anoxic marine sediments: implications for the geological record. Mar. Geol. 113, 67–88.

Campbell, L., Liu, H., Nolla, H.A., Vaulot, D., 1997. Annual variability of phytoplankton and bacteria in the subtropical North Pacific Ocean at Station ALOHA during the 1991–1994 ENSO event. Deep-Sea Res. 44, 167–192.

Canfield, D.E., 1994. Factors influencing organic carbon preservation in marine sediments. Chem. Geol. 114, 315–329.

Canfield, D.E., Thamdrup, B., Hansen, J.W., 1993a. The anaerobic degradation of organic matter in Danish coastal sediments: iron reduction, manganese reduction, and sulfate reduction. Geochim. Cosmochim. Acta 57, 3867–3883.

Canfield, D.E., Jørgensen, B.B., Fossing, H., Glud, R., Gundersen, J., Ramsing, N.B., Thamdrup, B., Hansen, J.W., Nielsen, L.P., Hall, P.O.J., 1993b. Pathways of organic carbon oxidation in three continental margin sediments. Mar. Geol. 113, 27–40.

Cao, C., Love, G.D., Hays, L.E., Wang, W., Shen, S., Summons, R.E., 2009. Biogeochemical evidence for euxinic oceans and ecological disturbance presaging the end-Permian mass extinction event. Earth Planet. Sci. Lett. 281, 188–201.

Chamot, D., Owttrim, G.W., 2000. Regulation of cold shock-induced RNA helicase gene expression in the cyanobacterium *Anabaena* sp. strain PCC 7120. J. Bacteriol. 182, 1251–1256.

Chen, L., Men, X., Ma, M., Li, P., Jiao, Q., Lu, S., 2010. Polysaccharide release by *Aphanothece halophytica* inhibits cyanobacteria/clay flocculation. J. Phycol. 46, 417–423.

Clarke, W.A., Konhauser, K.O., Thomas, J.C., Bottrell, S.H., 1997. Ferric hydroxide and ferric hydroxysulfate precipitation by bacteria in an acid mine drainage lagoon. FEMS Microbiol. Rev. 20, 351–361.

Cole, D.B., Reinhard, C.T., Wang, X., Gueguen, B., Halverson, G.P., Gibson, T., Hodgskiss, M.S.W., McKenzie, N.R., Lyons, T.W., Planavsky, N.J., 2016. A shale-hosted Cr istope record of low atmospheric oxygen during the Proterozoic. Geology 44, 555–558.

Condie, K.C., 2004. Supercontinents and superplume events: distinguishing signals in the geological record. Phys. Earth Planet. Inter. 146, 319–332.

Cox, J.S., Smith, D.S., Warren, L.A., Ferris, F.G., 1999. Characterizing heterogeneous bacterial surface functional groups using discrete affinity spectra for proton binding. Environ. Sci. Technol. 33, 4514–4521.

Crowe, S.A., Døssing, L.N., Beukes, N.J., Bau, M., Kruger, S.J., Frei, R., Canfield, D.E., 2013. Atmospheric oxygenation three billion years ago. Nature 501, 535–539.
Davis, C.C., Chen, H.W., Edwards, M., 2002. Modeling silica sorption to iron hydroxide. Environ. Sci. Technol. 36, 582–587.
Dean, W.E., 2007. Sediment geochemical records of productivity and oxygen depletion along the margin of western North America during the past 60,000 years: teleconnections with Greenland ice and the Cariaco Basin. Quat. Sci. Rev. 26, 98–114.
Dean, W.E., Gardner, J.V., Piper, D.Z., 1997. Inorganic geochemical indicators of glacial-interglacial changes in productivity and anoxia on the California continental margin. Geochim. Cosmochim. Acta 61, 4507–4518.
Ding, X., Henrichs, S.M., 2002. Adsorption and desorption of proteins and polyamino acids by clay minerals and marine sediments. Mar. Chem. 77, 225–237.
Dittrich, M., Sibler, S., 2005. Cell surface groups of two picocyanobacteria strains studied by zeta potential investigations, potentiometric titration, and infrared spectroscopy. J. Colloid Interface Sci. 286, 8.
Doyle, R.J., 1989. How cell walls of Gram-positive bacteria interact with metal ions. In: Beveridge, T.J., Doyle, R.J. (Eds.), Metal Ions and Bacteria. Wiley, New York, pp. 275–293.
Du, J., Pushkarova, R.A., Smart, R.St.C., 2009. A cryo-SEM study of aggregate and floc structure changes during clay settling and raking processes. Int. J. Miner. Process. 93, 66–72.
Dumitrescu, M., Brassell, S.C., 2005. Biogeochemical assessment of sources of organic matter and paleoproductivity during the early Aptian Oceanic Anoxic Event at Shatsky Rise, ODP Leg 198. Org. Geochem. 36, 1002–1022.
Duque-Botero, F., Maurrasse, F.J.-M.R., 2008. Role of cyanobacteria in Corg-rich deposits: an example from Indidura Formation (Cenomanian-Turonian), northeastern Mexico. 2008. Cretac. Res. 29, 957–964.
Ellis, A.S., Johnson, T.M., Bullen, T.D., 2002. Chromium isotopes and the fate of hexavalent chromium in the environment. Science 295, 2060–2062.
Ellis, A.S., Johnson, T.M., Bullen, T.D., 2004. Using chromium stable isotope ratios to quantify Cr(VI) reduction: lack of sorption effects. Environ. Sci. Technol. 38, 3604–3607.
Emerson, S., Hedges, J.I., 1988. Processes controlling the organic carbon content of open ocean sediments. Paléo 3, 621–634.
Fein, J.B., Daughney, C.J., Yee, N., Davis, T.A., 1997. A chemical equilibrium model for metal adsorption onto bacterial surfaces. Geochim. Cosmochim. Acta 61, 3319–3328.
Flemming, C.A., Ferris, F.G., Beveridge, T.J., Bailey, G.W., 1990. Remobilization of toxic heavy metals adsorbed to bacterial wall-clay composites. Appl. Environ. Microbiol. 56, 3191–3203.
Frei, R., Dahl, P.S., Frandsson, M.M., Jensen, L.A., Hansen, T.R., Terry, M.P., Frei, K.M., 2009. Lead-isotope and trace-element geochemistry of Paleoproterozoic metasedimentary rocks in the Lead and Rochford basins (Black Hills, South Dakota, USA): implications for genetic models, mineralization ages, and sources of leads in the Homestake gold deposit. Precambrian Res. 172, 1–24.
Glasauer, S., Langley, S., Beveridge, T.J., 2001. Sorption of Fe (hydr)oxides to the surface of *Shewanella putrefaciens*: cell-bound fine-grained minerals are not always formed de novo. Appl. Environ. Microbiol. 67, 5544–5550.
Guenther, M., Bozelli, R., 2004. Factors influencing algae-clay aggregation. Hydrobiologia 523, 217–223.
Hadjoudja, S., Deluchat, V., Baudu, M., 2010. Cell surface characterization of *Microcystis aeruginosa* and *Chlorella vulgaris*. J. Colloid Interface Sci. 342, 293–299.
Hamm, C.E., 2002. Interactive aggregation and sedimentation of diatoms and clay-sized lithogenic material. Limnol. Oceanogr. 47, 1790–1795.
Hedges, J.I., Keil, R.G., 1995. Sedimentary organic matter preservation: an assessment and speculative synthesis. Mar. Chem. 49, 81–115.
Herrle, J.O., Pross, J., Friedrich, O., Kössler, P., Hemleben, C., 2003. Forcing mechanisms for mid-Cretaceous black shale formation: evidence from the Upper Aptian and Lower Albian of the Vocontian Basin (SE France). Palaeogeogr. Palaeoclimatol. Palaeoecol. 190, 399–426.
Ho, T.-Y., Quigg, A., Finkel, Z.V., Milligan, A.J., Wyman, K., Falkowski, P.G., Morel, F.M.M., 2003. The elemental composition of some marine phytoplankton. J. Phycol. 39, 1145–1159.
Huang, K.-J., Teng, F.-Z., Wei, G.-J., Ma, J.-L., Bao, Z.-Y., 2012. Adsorption- and desorption-controlled magnesium isotope fractionation during extreme weathering of basalt in Hainan Island, China. Earth Planet. Sci. Lett. 359–360, 73–83.
Ikhsan, J., Johnson, B.B., Wells, J.D., 1999. A comparative study of the adsorption of transition metals on kaolinite. J. Colloid Interface Sci. 217, 403–410.
Izbicki, J.A., Ball, J.W., Bullen, T.D., Sutley, S.J., 2008. Chromium, chromium isotopes and selected trace elements, western Mojave Desert, USA. Appl. Geochem. 23, 1325–1352.
Jacquet, S., Lennon, J.-F., Marie, D., Vaulot, D., 1998. Picoplankton population dynamics in coastal waters of the northwestern Mediterranean Sea. Limnol. Oceanogr. 43, 1916–1931.
Jardillier, L., Zubkov, M.V., Pearman, J., Scanlan, D.J., 2010. Significant CO_2 fixation by small prymnesiophytes in the subtropical and tropical northeast Atlantic Ocean. ISME J. 4, 1180–1192.
Jia, C., Huang, J., Kershaw, S., Luo, G., Farabegoli, E., Perri, M.C., Chen, L., Bai, X., Xie, S., 2012. Microbial response to limited nutrients in shallow water immediately after the end-Permian mass extinction. Geobiology 10, 60–71.
Kashiyama, Y., Ogawa, N.O., Kuroda, J., Shiro, M., Nomoto, S., Tada, R., Kitazato, H., Ohkouchi, N., 2008. Diazotrophic cyanobacteria as the major photoautotrophs during mid-Cretaceous oceanic anoxic events: nitrogen and carbon isotopic evidence from sedimentary porphyrin. Org. Geochem. 39, 532–549.
Keil, R.G., Montluçon, D.B., Prahl, F.G., Hedges, J.I., 1994. Sorptive preservation of labile organic matter in marine sediments. Nature 370, 549–551.
Kelly, K.D., Benzel, W.M., Pfaff, K., 2013. Preliminary mineralogy and geochemistry of metal-rich (Mo-Ni-V-Zn) oil shale of the Carboniferous Heath Formation, Montana, USA. In: Jonsson, E. (Ed.), Mineral Deposit Research for a High-tech World. 12th SGA Biennial Meeting 2013. Proceedings. 2. pp. 636–639.
Kennedy, M.J., Pevear, D.R., Hill, R.J., 2002. Mineral surface control of organic carbon in black shale. Science 295, 657–660.
Kennedy, M.J., Löhr, S.C., Fraser, S.A., Baruch, E.T., 2014. Direct evidence for organic carbon preservation as clay-organic nanocomposites in a Devonian black shale; from deposition to diagenesis. Earth Planet. Sci. Lett. 388, 59–70.
Kim, C.J., Jung, Y.H., Ahn, C.Y., Lee, Y.K., Oh, H.M., 2010. Adsorption of turbid materials by the cyanobacterium *Phormidium parcydematicum*. J. Appl. Phycol. 22, 181–186.
Kilbertus, G., 1980. Microhabitats in soil aggregates their relationship with bacterial biomass and size of procaryotes present. Rev. Ecol. Biol. Sol 17, 543–557.
Kirby, R., Parker, W.R., 1983. Distribution and behavior of fine sediment in the Severn Estuary and Inner Bristol Channel, UK. Can. J. Fish. Aquat. Sci. 40 (Suppl. 1), 83–95.
Kistner, D.A., Pettigrew, N.R., 2001. A variable turbidity maximum in the Kennebec Estuary. Estuaries 24, 680–687.
Konhauser, K.O., 2007. Introduction to Geomicrobiology. Blackwell Publishing, Oxford, UK (425 pp.).
Konhauser, K.O., Urrutia, M.M., 1999. Bacterial clay authigenesis: a common biochemical process. Chem. Geol. 161, 399–413.
Konhauser, K.O., Fyfe, W.S., Ferris, F.G., Beveridge, T.J., 1993. Metal sorption and mineral precipitation by bacteria in two Amazonian river systems: Rio Solimões and Rio Negro. Geology 21, 1103–1106.
Konhauser, K.O., Fyfe, W.S., Schultze-Lam, S., Ferris, F.G., Beveridge, T.J., 1994. Iron phosphate precipitation by epilithic microbial biofilms in Arctic Canada. Can. J. Earth Sci. 31, 1320–1324.
Konhauser, K.O., Fisher, Q.J., Fyfe, W.S., Longstaffe, F.J., Powell, M.A., 1998. Authigenic mineralization and detrital clay binding by freshwater biofilms: the Brahmani river, India. Geomicrobiol J. 15, 209–222.
Köster, J., Rospondek, M., Schouten, S., Kotarba, M., Zubrzycki, A., Sinninghe Damsté, J.S., 1998. Biomarker geochemistry of a foreland basin: the Oligocene Menilite Formation in the Flysch Carpathians of southeast Poland. Org. Geochem. 29, 649–669.
Kristensen, E., 2000. Organic matter diagenesis at the oxic/anoxic interface in coastal marine sediments, with emphasis on the role of burrowing animals. Hydrobiologia 426, 1–24.
Krull, E.S., Baldock, J.A., Skjemstad, J.O., 2003. Importance of mechanisms and processes of the stabilization of soil organic matter for modeling carbon turnover. Funct. Plant Biol. 30, 207–222.
Kuypers, M.M.M., van Breugel, Y., Schouten, S., Erba, E., Sinninghe-Damsté, J.S.S., 2004. N2-fixing cyanobacteria supplied nutrient N for Cretaceous oceanic anoxic events. Geology 32, 853–856.
Lalonde, S.V., Smith, D.S., Owttrim, G.W., Konhauser, K.O., 2008a. Acid-base properties of cyanobacterial surfaces I: influences of growth phase and nitrogen metabolism on surface reactivity. Geochim. Cosmochim. Acta 72, 1257–1268.
Lalonde, S.V., Smith, D.S., Owttrim, G.W., Konhauser, K.O., 2008b. Acid-base properties of cyanobacterial surfaces II: silica as a chemical stressor influencing cell surface reactivity. Geochim. Cosmochim. Acta 72, 1269–1280.
Liu, Y.X., Alessi, D.S., Owttrim, G.W., Petrash, D.E., Mloszewska, A.M., Lalonde, S.V., Martinez, R.E., Zhou, Q.X., Konhauser, K.O., 2015. Cell surface reactivity of *Synechococcus* sp. PCC 7002: implications for metal sorption from seawater. Geochim. Cosmochim. Acta 169, 30–44.
Lünsdorf, H., Erb, R.W., Abraham, W.-R., Timmis, K.N., 2000. 'Clay hutches': a novel interaction between bacteria and clay minerals. Environ. Microbiol. 2, 161–168.
Ludwig, M., Bryant, D.A., 2012. Synechococcus sp. strain PCC 7002 transcriptome: acclimation to temperature, salinity, oxidative stress, and mixotrophic growth conditions. Front. Microbiol. 3, 1–14.
MacEachern, J.A., Pemberton, S.G., Gingras, M.K., Bann, K.L., 2010. Ichnology and facies models. In: Dalrymple, R.W., James, N.P. (Eds.), Facies Models 4, Geotext 6. Geological Association of Canada, St John's Nfld (586 pp.).
Mackin, J.E., Swider, K.T., 1989. Organic matter decomposition pathways and oxygen consumption in coastal marine sediments. J. Mar. Res. 47, 681–716.
Macquaker, H.S., Keller, M.A., Davies, S.J., 2010. Algal blooms and "marine snow": mechanisms that enhance preservation of organic carbon in ancient fine-grained sediments. J. Sediment. Res. 80, 934–942.
Mayer, L.M., Schick, L.L., Hardy, K.R., Wagal, R., MacCarthy, J., 2004. Organic matter in small mesopores in sediments and soils. Geochim. Cosmochim. Acta 68, 3863–3872.
McClure, R.S., Overall, C.C., McDermott, J.E., Hill, E.A., Markillie, L.-M., McCue, L.-A., Taylor, R.C., Ludwig, M., Bryant, D.A., Beliaev, A.S., 2016. Network analysis of transcriptomics expands regulatorylandscapes in *Synechococcus* sp. PCC 7002. Nucleic Acids Res. 44, 1–16.
Mitbavkar, S., Rajaneesh, K.M., Anil, A.C., Sundar, D., 2012. Picophytoplankton community in a tropical estuary: detection of *Prochlorococcus*-like populations. Estuar. Coast. Shelf Sci. 107, 159–164.
Miyazono, A., Odate, T., Maita, Y., 1992. Seasonal fluctuations of cell density of cyanobacteria and other picophytoplankton in Iwanai Bay, Hokkaido, Japan. J. Oceanogr. 48, 257–266.
Murphy, A.E., Sageman, B.B., Hollander, D.J., 2000. Eutrophication by decoupling of the marine biogeochemical cycles of C, N, and P: a mechanism for the Late Devonian mass extinction. Geology 28, 427–430.
Nuester, J., Vogt, S., Newville, M., Kustka, A.B., Twining, B., 2012. The unique biogeochemical signature of the marine diazotroph *Trichodesmium*. Front. Microbiol. 3 (article number 150).
Ockert, C., Gussone, N., Kaufhold, S., Teichert, B.M.A., 2013. Isotope fractionation during Ca exchange on clay minerals in a marine environment. Geochim. Cosmochim. Acta

112, 374–388.
Ohkouchi, N., Kashiyama, Y., Kuroda, J., Ogawa, N.O., Kitazato, H., 2006. The importance of diazotrophic cyanobacteria as primary producers during Cretaceous Oceanic Anoxia Event 2. Biogeosciences 3, 467–478.
Olcott, A.N., Sessions, A.L., Corsetti, F.A., Kaufman, A.J., de Oliviera, T.F., 2005. Biomarker evidence for photosynthesis during neoproterozoic glaciation. Science 310, 471–474.
Pan, L., Zhang, J., Zhang, L., 2007. Picophytoplankton, nanophytoplankton, heterotrophic bacteria and viruses in the Changjiang Estuary and adjacent coastal waters. J. Plankton Res. 29, 187–197.
Partin, C.A., Bekker, A., Planovsky, N.J., Scott, C.T., Gill, B.C., Li, C., Podkovyrov, V., Maslov, A., Konhauser, K.O., Lalonde, S.V., Love, G.D., Poulton, S.W., Lyons, T.W., 2013. Large-scale fluctuations in Precambrian atmospheric and oceanic oxygen levels from the record of U in shales. Earth Planet. Sci. Lett. 369, 284–293.
Pedersen, T.F., Calvert, S.E., 1990. Anoxia vs. productivity: what controls the formation of organic-carbon-rich sediments and sedimentary rocks? Am. Assoc. Pet. Geol. Bull. 74, 454–466.
Petrash, D.A., Gueneli, N., Brocks, J.J., Méndez, J.A., Gonzalez-Arismentdi, G., Poulton, S.W., Konhauser, K.O., 2016. Black shale deposition and early diagenetic dolomite cementation during Oceanic Anoxic Event 1: the mid-Cretaceous Maracaibo Platform, northwestern South America. Am. J. Sci. 316, 669–711.
Phoenix, V.R., Konhauser, K.O., 2008. Benefits of bacterial biomineralization. Geobiology 6, 303–308.
Phoenix, V.R., Martinez, R.E., Konhauser, K.O., Ferris, F.G., 2002. Characterization and implications of the cell surface reactivity of *Calothrix* sp. strain KC97. Appl. Environ. Microbiol. 68, 4827–4834.
Piper, D.Z., Calvert, S.E., 2009. A marine biogeochemical perspective on black shale deposition. Earth-Sci. Rev. 95, 63–96.
Piper, D.Z., Perkins, R.B., 2004. A modern vs. Permian black shale-the hydrography, primary productivity, and water-column chemistry of deposition. Chem. Geol. 206, 177–197.
Planavsky, N.J., Reinhard, C.T., Wang, X., Thomson, D., McGoldrick, P., Rainbird, R.H., Johnson, T., Fischer, W.W., Lyons, T.W., 2014. Low Mid-Proterozoic atmospheric oxygen levels and the delayed rise of animals. Science 346, 635–638.
Pokrovsky, O.S., Martinez, R., Golubev, S., Kompantseva, E., Shirokova, L., 2008. Adsorption of metals and protons on *Gloeocapsa* sp. cyanobacteria: a surface speciation approach. Appl. Geochem. 23, 2574–2588.
Porra, R.J., Thompson, W.A., Kriedemann, P.E., 1989. Determination of accurate extinction coefficients and simultaneous equations for assaying chlorophylls *a* and *b* extracted with four different solvents: verification of the concentration of chlorophyll standards by atomic absorption spectroscopy. Biochim. Biophys. Acta 975, 384–394.
Rajaneesh, K.M., Mitbavkar, S., 2013. Factors controlling the temporal and spatial variations in *Synechococcus* abundance in a monsoonal estuary. Mar. Environ. Res. 92, 133–143.
Ransom, B., Bennett, R.H., Baerwald, R., Shea, K., 1997. TEM study of in situ organic matter on continental margins: occurrence and the “monolayer” hypothesis. Mar. Geol. 138, 1–9.
Ransom, B., Kim, D., Kastner, M., Wainwright, S., 1998. Organic matter preservation on continental slopes: importance of mineralogy and surface area. Geochim. Cosmochim. Acta 62, 1329–1345.
Rao, R., Song, S., Lopez-Valdivieso, A., 2012. Specific adsorption of chromium species on kaolinite surface. Miner. Process. Extr. Metall. Rev. 33, 180–189.
Raven, J., Falkowski, P., 1999. Oceanic sinks for atmospheric CO_2. Plant Cell Environ. 22, 741–755.
Reinhard, C.T., Planavsky, N.J., Robbins, L.J., Partin, C.A., Gill, B.C., Lalonde, S.V., Bekker, A., Konhauser, K.O., Lyons, T.W., 2013. Proterozoic ocean redox and biogeochemical stasis. Proc. Natl. Acad. Sci. U. S. A. 110, 5357–5362.
Reinhard, C.T., Planavsky, N.J., Wang, X., Fischer, W.W., Johnson, T.M., Lyons, T.W., 2014. The isotopic composition of authogenic chromium in anoxic marine sediments: a case study from the Cariaco Basin. Earth Planet. Sci. Lett. 407, 9–18.
Sakamoto, T., Bryant, D.A., 1998. Growth at low temperature causes nitrogen limitation in the cyanobacterium *Synechococcus* sp. PCC 7002. Arch. Microbiol. 169, 10–19.
Schauble, E., Rossman, G.R., Taylor Jr., H.P., 2004. Theoretical estimates of equilibrium chromium-isotope fractionations. Chem. Geol. 205, 99–114.
Schultze-Lam, S., Fortin, D., Davies, B.S., Beveridge, T.J., 1996. Mineralization of bacterial surfaces. Chem. Geol. 132, 171–181.
Scott, C., Lyons, T.W., Bekker, A., Shen, Y., Poulton, S.W., Chu, X., Anbar, A.D., 2008. Tracing the stepwise oxidation of the Proterozoic ocean. Nature 452, 456–458.
Scott, C.T., Planavsky, N.J., Dupont, C.L., Kendall, B., Gill, B.C., Robbins, L.J., Husband, K.F., Arnold, G.L., Wing, B.A., Poulton, S.W., Bekker, A., Anbar, A.D., Konhauser, K.O., Lyons, T.W., 2013. Bioavailability of zinc in marine systems through time. Nat. Geosci. 6, 125–128.
Sengco, M.R., Li, A.S., Tugend, K., Kulis, D., Anderson, D.M., 2001. Removal of red- and brown-tide cells using clay flocculation I. Laboratory culture experiments with *Gymnodinium breve* and *Aureococcus anophagefferens*. Mar. Ecol. Prog. Ser. 210, 41–53.
Smith, S.V., Hollibaugh, 1993. Coastal metabolism and the oceanic organic carbon balance. Rev. Geophys. 31, 75–89.
Spark, K.M., Wells, J.D., Johnson, B.B., 1995. Eur. J. Soil Sci. 46, 633–640.
Stevens, S.E., Porter, R.D., 1980. Transformation in *Agmenellum quadruplicatum*. Proc. Natl. Acad. Sci. U. S. A. 77, 6052–6056.
Suess, E., 1980. Particulate organic carbon flux in the oceans – surface productivity and oxygen utilization. Nature 288, 260–262.
Sutherland, B.R., Barrett, K.J., Gingras, M.K., 2014. Clay settling in fresh and salt water. Environ. Fluid Mech. 15, 147–160.
Suzuki, N., Ishida, K., Shinomiya, Y., Ishiga, H., 1998. High productivity in the earliest Triassic ocean: black shales, Southwest Japan. Palaeogeogr. Palaeoclimatol. Palaeoecol. 141, 53–65.
Swanner, E.D., Planavsky, N.J., Lalonde, S.V., Robbins, L.J., Bekker, A., Rouxel, O.J., Saito, M.A., Kappler, A., Mojzsis, J., Konhauser, K.O., 2014. Cobalt and marine redox evolution. Earth Planet. Sci. Lett. 390, 253–263.
Taggart Jr., M.S., Kaiser, A.D. Junior, 1960. Clay mineralogy of the Mississippi River deltaic sediments. Geol. Soc. Am. Bull. 71, 521–530.
Thiry, M., 2000. Palaeoclimatic interpretation of clay minerals in marine deposits: an outlook from the continental origin. Earth Sci. Rev. 49, 201–221.
Thomas, F., Michot, L.J., Vantelon, D., Montarges, E., Prelot, B., Cruchaudet, M., Delon, J.-F., 1999. Layer charge and electrophoretic mobility of smectites. Colloids Surf. A Physicochem. Eng. Asp. 159, 351–358.
Tietjen, T., Vähätalo, A.V., Wetzel, R.G., 2005. Effects of clay mineral turbidity on dissolved organic carbon and bacterial production. Aquat. Sci. 67, 51–60.
Tribovillard, N., Algeo, T.J., Lyons, T., Riboulleau, A., 2006. Trace metals as paleoredox and paleoproductivity proxies: an update. Chem. Geol. 232, 12–32.
Twining, B.S., Baines, S.B., Fisher, N.S., 2004. Element stoichiometries of individual plankton cells collected during the southern ocean iron experiment (SOFeX). Limnol. Oceanogr. 49, 2115–2128.
Tyson, R.V., 2001. Sedimentation rate, dilution, preservation and total organic carbon: some results of a modeling study. Org. Geochem. 32, 333–339.
Uncles, R.J., Stephens, J.A., Law, D.J., 2006. Turbidity maximum in the macrotidal, highly turbid Humber Estuary, UK: flocs, fluid mud, stationary suspensions and tidal bores. Estuar. Coast. Shelf Sci. 67, 30–52.
Urrutia, M.M., Kemper, M., Doyle, R., Beveridge, T.J., 1992. The membrane-induced proton motive force influences the metal binding ability of *Bacillus subtilis* cell walls. Appl. Environ. Microbiol. 58, 3837–3844.
Verspagen, J.M.H., Visser, P.M., Huisman, J., 2006. Aggregation with clay causes sedimentation of the buoyant cyanobacteria *Microcystis* spp. Aquat. Microb. Ecol. 44, 165–174.
Walker, S.G., Flemming, C.A., Ferris, F.G., Beveridge, T.J., Bailey, G.W., 1989. Physiochemical interaction of *Escherichia coli* cell envelopes and *Bacillus subtilis* cell walls with two clays and ability of the composite to immobilize heavy metals from solution. Appl. Environ. Microbiol. 55, 2976–2984.
Wan, S., Li, A., Clift, P.D., Stuut, J.-B.W., 2007. Development of the East Asian monsoon: mineralogical and sedimentological records in the northern South China Sea since 20 Ma. Palaeogeogr. Palaeoclimatol. Palaeoecol. 254, 561–582.
Wanty, R.B., Goldhaber, M.B., 1992. Thermodynamics and kinetics of reactions involving vanadium in sedimentary rocks. Geochim. Cosmochim. Acta 56, 1471–1483.
Waterbury, J.B., Watson, S.W., Guillard, R. R. L. And Brand, L. E., 1979. Widespread occurrence of a unicellular, marine, planktonic, cyanobacterium. Nature 277, 293–294.
Xie, S., Pancost, R.D., Yin, H., Wang, H., Evershed, R.P., 2005. Two episodes of microbial change coupled with Permo/Triassic faunal mass extinction. Nature 434, 494–497.
Xu, L., Lehmann, B., Mao, J., Nägler, T.F., Neubert, N., Böttcher, M.E., Escher, P., 2012. Mo isotope and trace element patterns of Lower Cambrian black shales in South China: multi-proxy constraints on the paleoenvironment. Chem. Geol. 318–319, 45–59.